Accepted Manuscript

Design, synthesis and biological evaluation of tetrazole-containing RXRα ligands as anticancer agents

Zhiqiang Yan, Shuyi Chong, Huiyun Lin, Qian Yang, Xin Wang, Weidong Zhang, Xiaokun Zhang, Zhiping Zeng, Ying Su

PII: S0223-5234(18)31073-0

DOI: https://doi.org/10.1016/j.ejmech.2018.12.036

Reference: EJMECH 10969

To appear in: *European Journal of Medicinal Chemistry*

Received Date: 30 September 2018

Revised Date: 11 December 2018

Accepted Date: 14 December 2018

Please cite this article as: Z. Yan, S. Chong, H. Lin, Q. Yang, X. Wang, W. Zhang, X. Zhang, Z. Zeng, Y. Su, Design, synthesis and biological evaluation of tetrazole-containing RXRα ligands as anticancer agents, *European Journal of Medicinal Chemistry* (2019), doi: https://doi.org/10.1016/j.ejmech.2018.12.036.

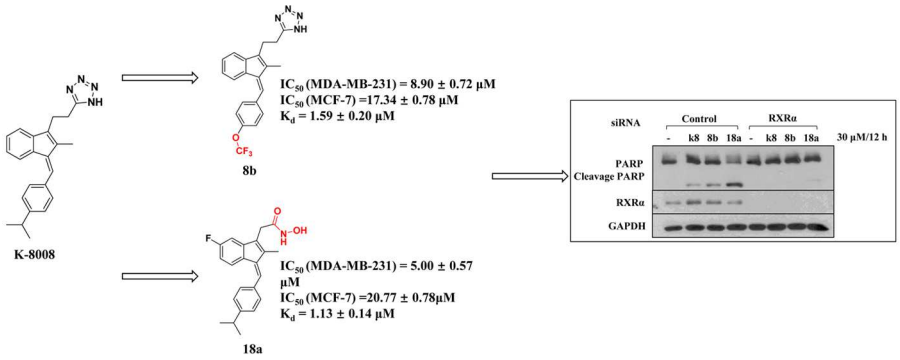

Design, synthesis and biological evaluation of tetrazole-containing RXRα ligands as anticancer agents

Zhiqiang Yan [a, 1], *Shuyi Chong* [a, 1], *Huiyun Lin* [a, 1], *Qian Yang* [a], *Xin Wang* [a], *Weidong Zhang* [a], *Xiaokun Zhang* [a, b], *Zhiping Zeng* [a, *], *Ying Su* [b, *].

[a] *School of Pharmaceutical Science, Fujian Provincial Key Laboratory of Innovative Drug Target Research, Xiamen University, Fujian, 361002, China*

[b] *Sanford Burnham Prebys Medical Discovery Institute, 10901 N. Torrey Pines Road, La Jolla, CA 92037, USA*

[1] *These authors contributed equally to this work.*

[*] *To whom correspondence should be addressed:*

Email: ysu@sbpdiscovery.org (Y. Su) or to zengzhiping@xmu.edu.cn (Z. Zeng)

Abstract:

Nuclear receptor RXRα plays an important role in many biological and pathological processes. The nongenomic action of RXRα is implicated in many cancers. K-8008, a non-canonical RXRα ligand derived from sulindac, inhibits the TNFα-activated PI3K/AKT pathway by mediating the interaction between a truncated form of RXRα (tRXRα) and the p85α regulatory subunit of PI3K and exerts potent anticancer activity in animal model. Herein we report our studies of a novel series of K-8008 analogs as potential anticancer agents targeting RXRα. Two compounds **8b** and **18a** were identified to have slightly stronger binding to RXRα and improved apoptotic activities in breast cancer cells.

Key words: RXRα; RXRα modulator; PI3K/AKT pathway; Anticancer activity; bioisostere.

1. Introduction

As a unique and important member of the nuclear receptor (NR) superfamily, retinoid X receptor-α (RXRα) plays critical roles in many biological and pathological processes [1]. Dysfunctions of RXRα are implicated in a number of diseases, such as cancer [2]. Targeted disruption of RXRα gene leads to prostatic preneoplastic lesions [3] and skin abnormalities [4].

RXRα exhibits a modular organization structurally consisting of three main functional domains: an N-terminal region, a DNA binding domain, and a ligand-binding domain (LBD). The LBD is composed of a ligand-binding pocket (LBP) for binding small molecule ligands; a transactivation function domain termed AF-2 composed of helix 12 (H12) of the LBD, a co-regulator binding surface, and a dimerization surface [5, 6]. A well-studied mechanism of NR action is the ligand-mediated transcriptional regulation. Ligand binding to the LBP induces the conversion of the corepressor-binding site into a coactivator-binding site that triggers a cascade of events and leads to biological activities. Thus, RXRα is widely studied for its action as a

ligand-mediated transcription factor and many molecules have been reported to bind to the LBP of RXRα. In general, RXRα LBD ligands are constituted of three important aspects, including a polar motif head, such as carboxyl group, a central polyene linker and a hydrophobic tail [7, 8]. The 9-*cis* retinoic acid (9-*cis*-RA) is identified as an endogenous RXRα ligand. Targretin, an RXR-selective ligand, acts as a highly effective agent for mammary carcinoma and is approved by FDA to treat cutaneous T-cell lymphoma [9, 10].

Besides acting as a transcription factor, RXRα possesses important extracellular functions [11-15]. We previously discovered that RXRα and its ligands can directly modulate the PI3K/AKT survival pathway in a TNFα-dependent manner. TNFα is a multifunctional cytokine that controls diverse cellular events such as cell survival and death that control the destiny of cancer cells [16]. PI3K/AKT activation is implicated in oncogenesis and drug resistance. Aberrations in this pathway can potentially cause cell transformation, metabolic disorders, and neurodegenerative diseases, as well as drug resistance [17]. The pathway has therefore been targeted extensively for therapeutic application. However, strategies that rely on direct inhibition of PI3K/AKT activities are hindered by toxicity or lack of selectivity [18]. Thus, identifying key molecules involved in the aberrant PI3K/AKT activation could offer new strategies for drug development. We found that an N-terminally truncated RXRα (tRXRα), detected in a variety of cancer cell lines, could act to mediate TNFα activation of PI3K/AKT in a number of cancer cell lines [19]. tRXRα is cytoplasmic and interacts with the p85α subunit of PI3K to activate the PI3K/AKT survival pathway and induce anchorage-independent cell growth *in vitro* and cancer cell growth in animals. Therefore, this nongenomic regulation of the PI3K/AKT signaling pathway by tRXRα provides new strategies to inhibit the activation of PI3K/AKT in cancer cells by targeting RXRα.

We found that K-8008 (Fig. 1), a derivative of sulindac, can bind tRXRα and mediate the interaction between tRXRα and p85α regulatory subunit of PI3K, leading to the inhibition of the TNFα-activated PI3K/AKT pathway [19-21]. In animal experiments, K-8008 effectively inhibited the growth of tumor, implying that K-8008 could be a potential anticancer lead. Furthermore, the

crystal structure of the K-8008 bound RXRα-LBD reveals a new binding mode, which is different from the canonical ligand binding in the LBP. Thus, K-8008 represents a new class of RXRα ligands. Here we report the design, synthesis and biological evaluation of a series of K-8008 derivatives. A total of 26 compounds were synthesized, and their apoptotic activity, binding activity and SAR were investigated. Two compounds **8b** and **18a** displayed improved apoptotic activities in breast cancer cells.

2. Chemistry

The proposed K-8008 derivatives were synthesized according to **Schemes 1-4**. Compounds **8a-k** and compound **9a** were prepared using Scheme 1. Under the treatment of K_2CO_3 as a catalytic base, benzaldehyde **1** reacted with propionic anhydride (**2a**) or acetic anhydride (**2b**) at 140 °C overnight to afford **2a** in 83% yield and **2b** in 60% yield. **2a-b** was reduced by hydrogen gas catalyzed by Pd/C at room temperature in methanol for 16 h to afford **3a-b** in about 90% yield. **4a-b** were prepared from **3a-b** using polyphosphoric acid (PPA) as the condensing agent at 80 °C for 4 h. With the help of samarium (II) iodide in THF solution also known as "Kagan's reagent", indanone **4a-b** successfully coupled with acrylonitrile and the product mixtures were processed with a solution of H_2SO_4 and HOAc (v/v= 10:1) to afford **5a** and **5b** in 20% to 55% yields. The obtained cyano products **5a-b** were reacted with sodium azide, catalyzed by triethylamine hydrochloride in DMF to form the tetrazole products **6a** (84%) and **7a** (56%), respectively. For step vi. sodium methoxide was used as the base for the condensation reaction of compound **6a** or **7a** with different substituted aromatic aldehydes to afford compounds **8a-k** and compound **9a.** The stereochemistry of this condensation is dictated by the presence of a R_1 group [22]. When R_1 = -CH_3, Z-isomers are the main products. Whereas R_1 = -H, E-isomers are the key products. Compound **13a** was prepared using scheme 2. Compound **4a** was treated with diethyl cyanethylphosphonate in the presence of DBU as catalyst to afford **10a** in 75% yield. Formation of **11** was easily achieved by reacting **10a** with hydroxylamine (50% wt in water) in the absence of catalyst. With the treatment of CDI and in

the presence of DBU as catalyst, **11** underwent ring closure to give the 4H-1,2,4-oxadiazol product **12**. Product **13a** was finally obtained by the condensation of 12 with aromatic aldehyde. Scheme 3 was used to make compound **17a** and **18a**. Reformatsky reaction was applied to introduce a methyl carboxylate into fluorinated indanone **14** with active zinc powder, α-bromide ester, and a mixture of MeOH and 1N NaOH solution (v/v= 4:3) to form carboxylic acid **15** in 52% yield. **16** was synthesized by the condensation reaction with 4-isopropylbenzaldehyde. **16** was subsequently amidated by reagent Amino-1H-tetrazole and catalyst EDCI/HOBT in CH_2Cl_2 at room temperature for 12 h to give product **17a** in 87% yield. To form compound **18a**, compound **16** was reacted with EtOH in the presence of catalyst H_2SO_4 and without further purification, and the products were kept on reacting with hydroxylamine to give **18a**. The final products (compounds **20a-i** and **21a-b)** were afforded using **Scheme 4** which is similar to **Scheme 1**. All the synthesized compounds were structurally elucidated by different spectrometric methods, including ^{1}H NMR (600 MHz), ^{13}C NMR (151 MHz) and HRMS (ESI) (see the spectra in the supporting information).

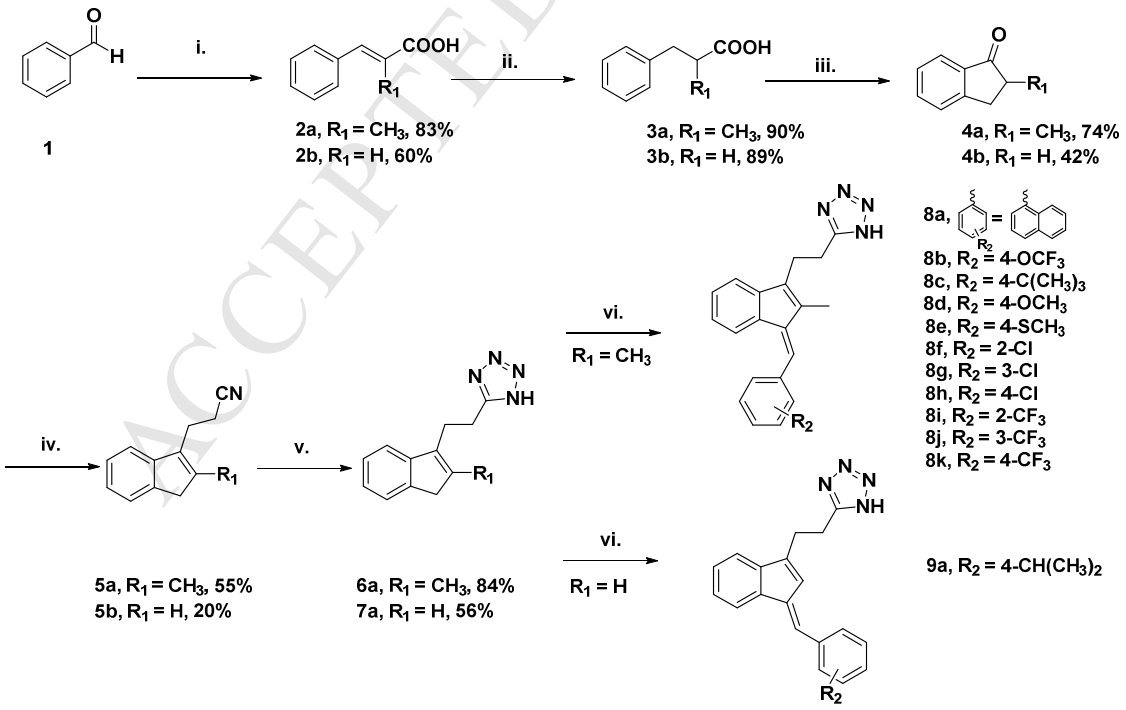

Scheme 1. Reagents and conditions. (i) Acetic anhydride or propionic anhydride, K_2CO_3, 140 °C, overnight; (ii) H_2/Pd-C, MeOH, r. t., 16 h; (iii) PPA, 80 °C, 4 h; (iv) samarium (II) iodide, acrylonitrile, isopropyl alcohol, THF, 0 °C, 20 min; AcOH, H_2SO_4, r. t., overnight; (v) sodium azide, triethylamine hydrochloride, DMF, 100 °C, 24 h; (vi) R_2-PhCHO, sodium methoxide, MeOH, 80 °C, 4 h, 41%~95%.

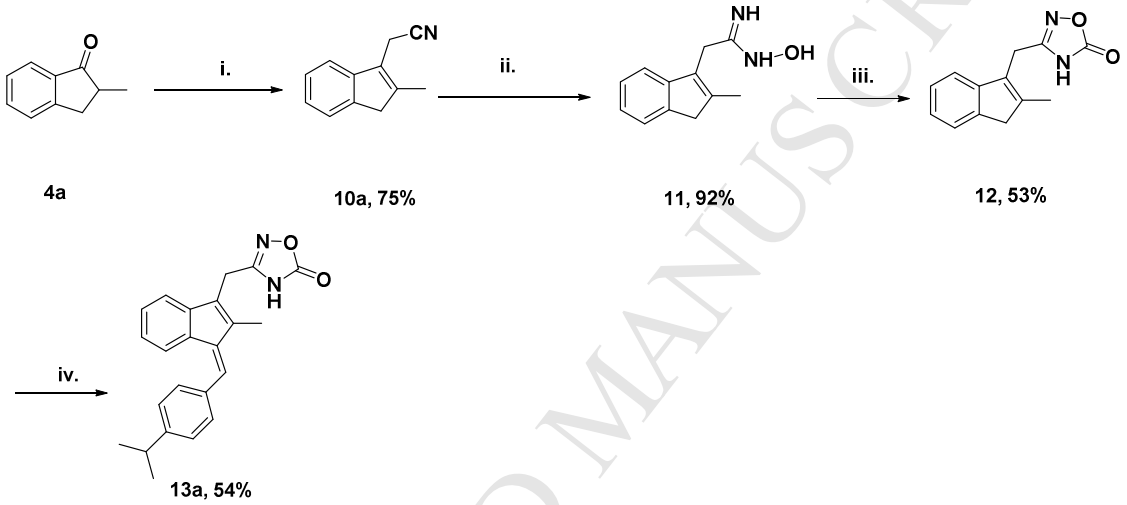

Scheme 2. Reagents and conditions. (i) diethyl cyanethylphosphonate, DBU, acetonitrile, r. t., 18 h;(ii) hydroxylamine (50% wt in water), EtOH, 80 °C, 3 h; (iii) CDI, DBU, 1,4-dioxane, 100 °C, 4 h; (iv) 4-isopropylbenzaldehyde, sodium methoxide, MeOH, 80 °C, 4 h.

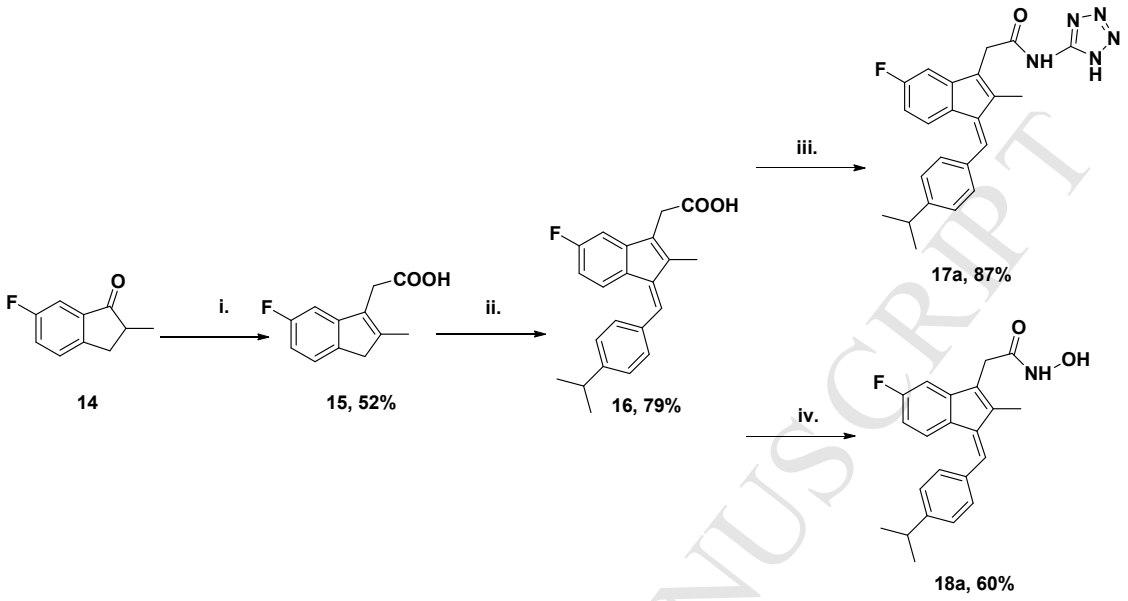

Scheme 3. Reagents and conditions. (i) ethyl bromoacetate, zinc powder, iodine, THF, 60 °C, 4 h; NaOH, MeOH, r. t., overnight; (ii) 4-isopropylbenzaldehyde, sodium methoxide, MeOH, 80 °C, 4 h; (iii) amino-1H-tetrazole, EDCI, HOBT, CH_2Cl_2, 0 °C - r. t., 12 h. (iv) H_2SO_4, EtOH, 60 °C, 2 h; hydroxylamine, sodium methoxide, MeOH, r. t., 4 h (two steps).

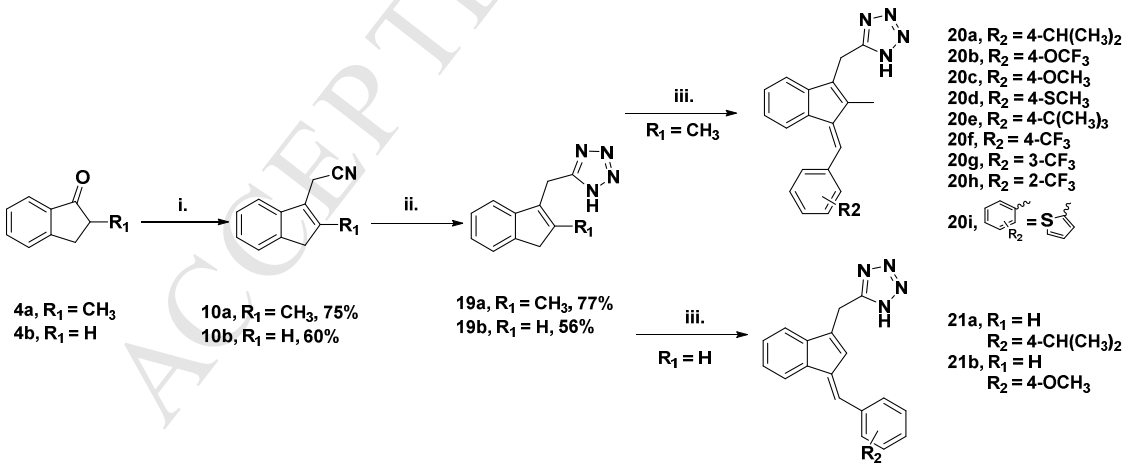

Scheme 4. Reagents and conditions. (i) diethyl cyanethylphosphonate, DBU, acetonitrile, r.t., 18 h; (ii) sodium azide, triethylamine hydrochloride, DMF, 110 °C, 40 h; (iii) R_2-PhCHO, sodium methoxide, MeOH, 80 °C, 4 h, 29%~57%.

3. Results and Discussion

3.1 Design of K-8008 derivatives

Previously we determined the crystal structure of RXRα-LBD/K-8008 complex and identified the binding mode of K-8008 in the LBD of RXRα (PBD code: 4N8R) [20]. In the crystal structure, two separate K-8008 molecules bind to the dimers of the RXRα tetramer. Each K-8008 is located in a region close to the dimer-dimer interface (Fig. 2A). The tetrazole motif of K-8008 plays an important role by anchoring the ligand via making charge-dipole interaction with Helix 11. The rigid indene portion of the ligand is tightly imbedded in a hydrophobic environment (Fig. 2B). However, there is considerable space around the R_2-benzene ring (Fig. 2B and Table 1.), offering opportunity to introduce substituents on the R_2-benzene ring to improve the binding affinity of the ligands. Therefore, we first focused on exploring different substituents on the R_2-benzene ring. 11 compounds **8a-k** were designed and synthesized as series 1. Previously we also reported that an E-isomer of K-80003 (Fig. 1) [21], compound **30** exerted enhanced binding activity compared to K-80003. Thus, we also made an E-isomer **9a** of K-8008 (as series 2 in Table 1.). Furthermore, K-8008 was developed based on K-80003 using the bioisostere concept and so we asked if tetrazole could be replaced by other bioisosteres. Three bioisosteres of K-8008 were synthesized as compounds **13a**, **17a** and **18a** (series 3 in Table 2, Scheme 2 and 3).

Recently we reported the crystal structure of K-80003 bound to RXRα-LBD and discovered that the binding mode of K-80003 is different from the binding mode of K-8008 (Fig. 2B). In the complex structure of RXRα-LBD with K-80003, three molecules of K-80003 bind to the same large hydrophobic cavity where only one molecule of K-8008 is bound in the crystal structure of RXRα-LBD/K-80008 complex (Fig. 2C-D) [23]. The difference in the binding modes between K-80003 and K-8008 could be due to the length of the linker between the charged group and the indene ring or to the difference in the nature of the charged groups. To have a better understanding

of the role of the linking length, compounds **20a-i** (series 4, in Table 3 and Scheme 4) and **21a-b** (series 5, in Table 3 and Scheme 4) were designed and synthesized for biological evaluation.

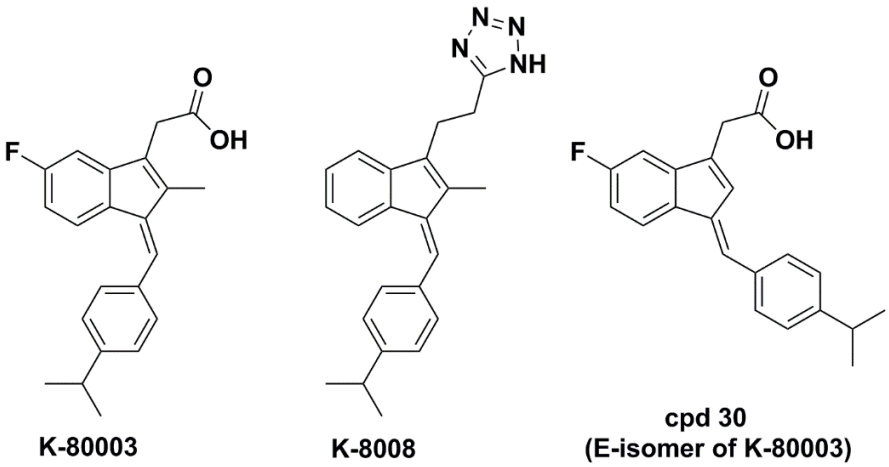

Fig 1. The chemical structures of K-80003, K-8008 and cpd 30.

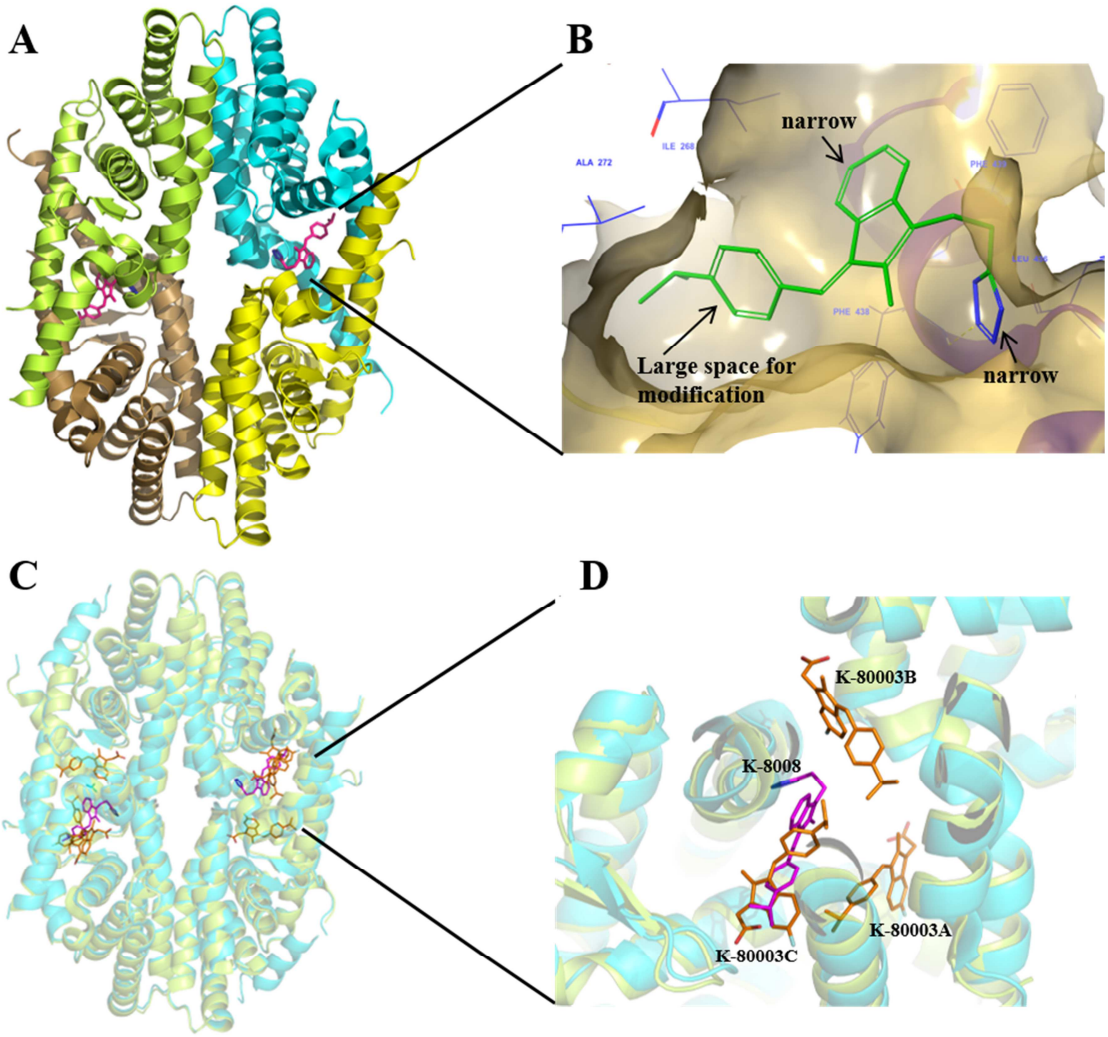

Fig 2. Crystal structures of RXRα-LBD in complex with K-8008 and K-80003. (A) Crystal Structure of RXRα-LBD in complex with K-8008 (PBD code: 4N8R) reveals that two K-8008 molecules bind to the dimers of the RXRα-LBD tetramer. The K-8008 molecules are shown in magenta sticks and the tetramer structure is shown in ribbon drawing. (B) Interactions between K-8008 and RXRα-LBD. K-8008 molecule is displayed in green sticks with its binding region in surface representation. (C) and (D) Superposition of the crystal structures of RXRα-LBD/K-80003 (PBD code: 5TBP) and RXRα-LBD/K-8008 (PBD code: 4N8R). The ribbon drawing of RXRα-LBD/K-80003 are displayed in yellow and the K-80003 molecules are in orange sticks. The

ribbon drawing of RXRα-LBD/K-8008 are displayed in cyan and the K-8008 molecules are in magenta sticks.

3.2 Antagonism activity of K-8008 derivatives

The synthesized compounds were first evaluated for their effects on RXRα transactivation activity by employing RXRα-LBD reporter assay. The LBD of RXRα was cloned as a Gal4 fusion and the resulting Gal4-RXRαLBD chimera and Gal4 reporter system were used to evaluate the effect of synthesized compounds. Gal4-RXRα/LBD strongly activated the Gal4 reporter in the presence of 9-*cis*-RA. Compounds were tested for their ability to inhibit the transactivation of 9-*cis*-RA at three different concentrations (1 μM, 10 μM and 50 μM). Compounds that demonstrated inhibition effects in a dose-dependent manner (Table 1-3) were considered to possess antagonism activity and were further evaluated for their anticancer activities. Among the 26 derivatives, 15 compounds displayed the dose-dependent inhibition of 9-*cis*-RA-induced reporter activity of RXRα.

3.3 In vitro anticancer activity and SAR study

The 15 compounds that could inhibit the RXRα transcription activity in dose-dependent manner were then evaluated for their growth inhibition of breast cancer cells in 2 cancer cell lines, MBA-MD-231 and MCF-7, using K-8008 as a positive control. Results are listed in Tables 1, 2 and 3. Based on the obtained data, structure-activity relationship was analyzed and summarized in Figure 3.

For compound series 1 (Table 1), we mainly focused on exploring different substituents on the R_2-benzene ring to study their structure-activity relationship. Firstly, larger steric hindrance group such as naphthalene ring (**8a**) was introduced to fill the available space where the R_2-benzene group binds as described in figure 2A, but surprisingly the compound failed to dose-dependently inhibit the transcriptional activity (see the supporting information S1). This result probably indicated that

simultaneous modification with large steric hindrance group at the *ortho* and *meta* position of the R_2-benzene ring was not in favor. Modifications with *tert*-butyl group (**8c**) slightly larger than the isopropyl group as in K-8008 at the *para* position maintained its antagonism activity (see the supporting information S1) but did not enhance its apoptotic activity against breast cancer cell(Table 1, **8c**). Compound **8b** where a slightly smaller but electron-withdrawing and high lipophilicity group trifluoromethoxy was used at the *para* position had also no reduction in its inhibition of the RXRα transcriptional activity (see the supporting information S1) but mildly enhanced its apoptotic effect against MDA-MB-231 and MCF-7(IC_{50} = 8.90 ± 0.72 μM and 17.34 ± 0.78 μM respectively) (Table 1, **8b**). Introduction of other electron-withdrawing groups such as trifluoromethyl and chlorine (**8h** and **8k**) at the *para* position of the R_2-benzene moiety could still maintain the compounds' antagonism activity (see the supporting information S2) but unfortunately displayed weaker apoptotic activity. On the contrary, electron-donating groups such as methoxy or methylthiol group (**8d** and **8e**) failed to work, with diminished antagonism effect (see the supporting information S1-2 and Table 1). Thus, it appears that the *para* position of the R_2-benzene ring prefers substituents with appropriate size (**K-8008**, **8c**) and electron-withdrawing groups (**8b**, **8h**, **8k**). For the *meta* position of R_2-benzene moiety, similar biological effects like **8h** and **8k** were observed when trifluoromethyl or chlorine (**8j** or **8g**) was introduced. Compounds **8f** and **8i** with R_2 = Cl and CF_3 respectively at the *Ortho*-position showed abolished activity (see the supporting information S2), implying that the *Ortho*-position of R_2-benzene cannot tolerate any substituents. For series 2 (Table 1.), the *E*-isomer product (**9a**) also reserved its antagonism activity (see the supporting information S3) but had a reduced apoptosis effect.

For series 3 (Table 2.), when the tetrazole group was transformed to oxadiazol and the length between polar group and indene moiety was changed from ethyl to methyl, the antagonism activity of compound **13a** was reserved (see the supporting information S3) and its apoptotic effect in MDA-MB-231 cancer cell was slightly improved from 12.34 ± 0.85 μM **(K-8008)** to 9.04 ± 1.06 μM (**13a**). The improvement in the apoptotic effect was also observed for compound **20a** (8.48 ±

0.68 μM in MDA-MB-231) where its oxadiazol was restored to tetrazole (**20a** in Table 3.). When a longer linker was used (**17a**), the compound did not show any apoptotic activities (Table 3.). although its antagonism activity was retained (see the supporting information S3). Compound **18a** resulted from substituting the tetrazole of compound **17a** with a carboxamide displayed an enhanced apoptotic effect. As evidenced from the IC_{50} values, compound **18a** was 2.5-fold (5.00 ± 0.57 μM) more potent than K-8008 in MDA-MB-231 cancer cell line and 1.3-fold (20.77 ± 0.78 μM) more potent than K-8008 in MCF-7.

We then changed the linking length between polar group and indene moiety from ethyl to methyl and evaluated the effect of different substituents on R_2-benzene moiety (series 4, Table 3). It is interesting to find that compounds of series 4 behaved differently from series 1. Modification at *para* position was not in favor of electron-withdrawing group such as trifluoromethoxy or trifluoromethyl (**20b** or **20f**). In addition, introduction of electron donating or aliphatic groups such as methoxy and tertiary butyl (**20c** and **20e**) did not result in improved apoptotic activity. Unlike compounds of series 1, when trifluoromethyl was introduced at *para*, *meta* or *ortho* position respectively, only substitution at *ortho* position (**20h**) could maintain its antagonism and apoptotic activity. The difference in the structure-activity relationship between series 1 and series 4 suggested that compounds of series 4 bind to RXRa differently from compounds of series 1. Furthermore, replacing R_2-benzene moiety with thiophene lost its apoptotic effect (**20i**). Two *E*-isomers (**21a** and **21b**) as series 5 were made and evaluated. Both **21a** and **21b** did not display any obvious antagonistic effect (Table 3.).

Table 1. The growth inhibition (IC_{50}, μM) of series 1 and 2 compounds against MDA-MB-231 and MCF-7.

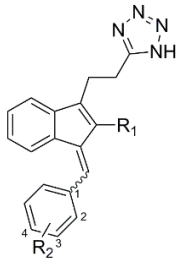

Compound	R_1	R_2	isomer	Reporter Assay[a]	MDA-MB-231[b]	MCF-7[b]
K-8008	CH_3	4-$CH(CH_3)_2$	Z	D[c]	12.34 ± 0.85	26.99 ± 3.78
8a		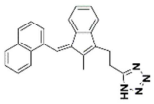	Z	ND[c]	NT[c]	NT[c]
8b	CH_3	4-OCF_3	Z	D[c]	8.90 ± 0.72	17.34 ± 0.78
8c	CH_3	4-$C(CH_3)_3$	Z	D[c]	12.49 ± 1.51	31.10 ± 1.29
8d	CH_3	4-OCH_3	Z	ND[c]	NT[c]	NT[c]
8e	CH_3	4-SCH_3	Z	ND[c]	NT[c]	NT[c]
8f	CH_3	2-Cl	Z	ND[c]	NT[c]	NT[c]
8g	CH_3	3-Cl	Z	D[c]	24.73 ± 0.33	45.55 ± 3.61
8h	CH_3	4-Cl	Z	D[c]	15.24 ± 1.73	56.29 ± 5.00
8i	CH_3	2-CF_3	Z	ND[c]	NT[c]	NT[c]
8j	CH_3	3-CF_3	Z	D[c]	15.58 ± 2.42	28.76 ± 4.62
8k	CH_3	4-CF_3	Z	D[c]	22.08 ± 1.54	39.36 ± 3.67
9a	H	4-$CH(CH_3)_2$	E	D[c]	15.57 ± 1.29	41.78 ± 5.34

[a]Reporter assay. Cells were incubated with corresponding compounds of 3 concentrations 1 μM, 10 μM and 50 μM. Compounds were tested for its dose-dependent antagonism activity.

[b]MTT methods. Cells were incubated with corresponding compounds at a concentration from 0.195 μM to 100 μM for 48 h. Compounds were tested for its IC_{50} value. Values are mean of three independent experiments.

[c]D: Dependent; ND: Not dependent; NT: Not tested.

Table 2. The growth inhibition (IC_{50}, μM) of series 3 compounds against MDA-MB-231 and MCF-7.

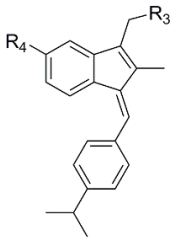

Compound	R_3	R_4	Reporter Assay[a]	MDA-MB-231[b]	MCF-7[b]
13a	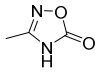	H	D[c]	9.04 ± 1.06	23.75 ± 1.67
17a	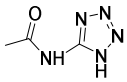	F	D[c]	NT[c]	NT[c]
18a	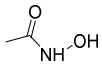	F	D[c]	5.00 ± 0.57	20.77 ± 0.78

[a]Reporter assay. Cells were incubated with corresponding compounds of 3 concentrations 1 μM, 10 μM and 50 μM. Compounds were tested its dose-dependent antagonism activity.

[b]MTT methods. Cells were incubated with corresponding compounds at a concentration from 0.195 μM to 100 μM for 48 h. Compounds were tested its IC_{50} value. Values are mean of three independent experiments.

[c]D: Dependent; ND: Not dependent; NT: Not tested.

Table 3. The growth inhibition (IC_{50}, μM) of series 4 and 5 compounds against MDA-MB-231 and MCF-7.

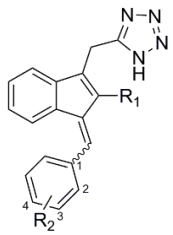

Compound	R_1	R_2	isomer	Reporter Assay[a]	MDA-MB-231[b]	MCF-7[b]
20a	CH_3	4-$CH(CH_3)_2$	Z	D[c]	8.48 ± 0.68	27.61 ± 1.64
20b	CH_3	4-OCF_3	Z	ND[c]	NT[c]	NT[c]
20c	CH_3	4-OCH_3	Z	D[c]	25.72 ± 0.82	104.00 ± 7.39
20d	CH_3	4-SCH_3	Z	ND[c]	NT[c]	NT[c]
20e	CH_3	4-$C(CH_3)_3$	Z	D[c]	14.33 ± 0.49	38.39 ± 1.708
20f	CH_3	4-CF_3	Z	ND[c]	NT[c]	NT[c]
20g	CH_3	3-CF_3	Z	ND[c]	NT[c]	NT[c]
20h	CH_3	2-CF_3	Z	D[c]	40.80 ± 3.10	62.28 ± 11.40
20i	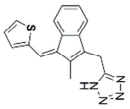		Z	D[c]	53.29 ± 2.81	124.5 ± 11.11
21a	H	4-$CH(CH_3)_2$	E	ND[c]	NT[c]	NT[c]
21b	H	4-OCH_3	E	ND[c]	NT[c]	NT[c]

[a]Reporter assay. Cells were incubated with corresponding compounds of 3 concentrations 1 μM, 10 μM and 50 μM. Compounds were tested its dose-dependent antagonism activity.

[b]MTT methods. Cells were incubated with corresponding compounds at a concentration from 0.195 μM to 100 μM for 48 h. Compounds were tested its IC_{50} value. Values are mean of three independent experiments.

[c]D: Dependent; ND: Not dependent; NT: Not tested.

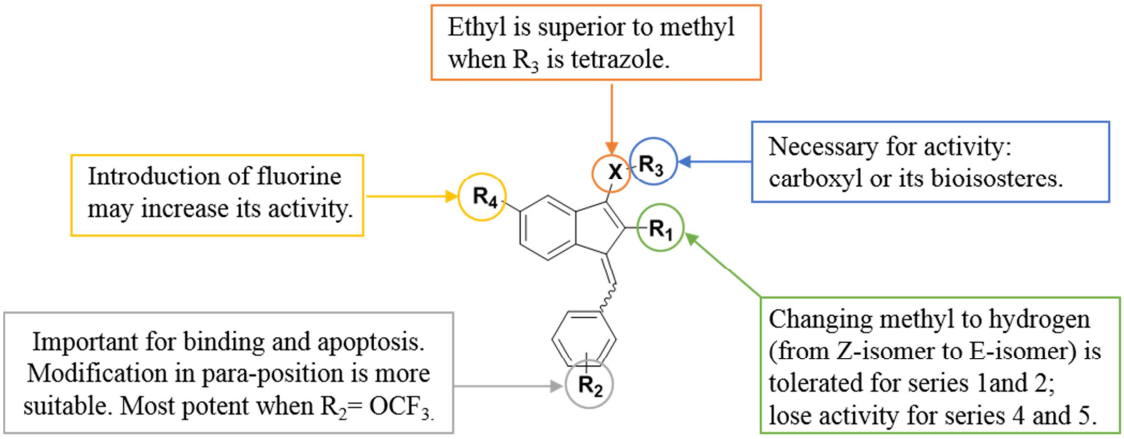

Fig 3. Summary of the structure-activity relationship.

3.4 The binding affinity of K-8008 derivatives

Fluorescence quenching assay was utilized to analyze the binding property of K-8008 derivatives. The compounds were titrated into the cuvette filled with a RXRα-LBD protein solution (1 μmol/L) with an increasing concentration from 0.5 μmol/L to 35 μmol/L. The fluorescence absorption excited by RXRα-LBD was quenched due to the interaction between the protein and compounds. We used K-80003 as a positive control that was reported before as a unique RXRα modulator with a dissociation constant (K_d) of 2.4 μM by means of 9-*cis*-RA competition binding assay [21]. Using the fluorescence quenching assay, the dissociation constant of K-80003 was evaluated as 2.38 ± 0.17 μM (Fig. 4A), which is consistent with the data from the 9-*cis*-RA competition binding assay. We then measured the dissociation constant (K_d) of three compounds (**K-8008**, **8b** and **18a**) that exerted enhanced apoptotic activity. K_d of 2.05 ± 0.26 μM, 1.59 ± 0.20 μM and 1.13 ± 0.14 μM were obtained for **K-8008**, **8b** and **18a** respectively (Fig. 4). The results showed that both of **8b** and **18a** bind to RXRα slightly better than K-8008 which was consistent with the apoptotic activity results from the MTT assay.

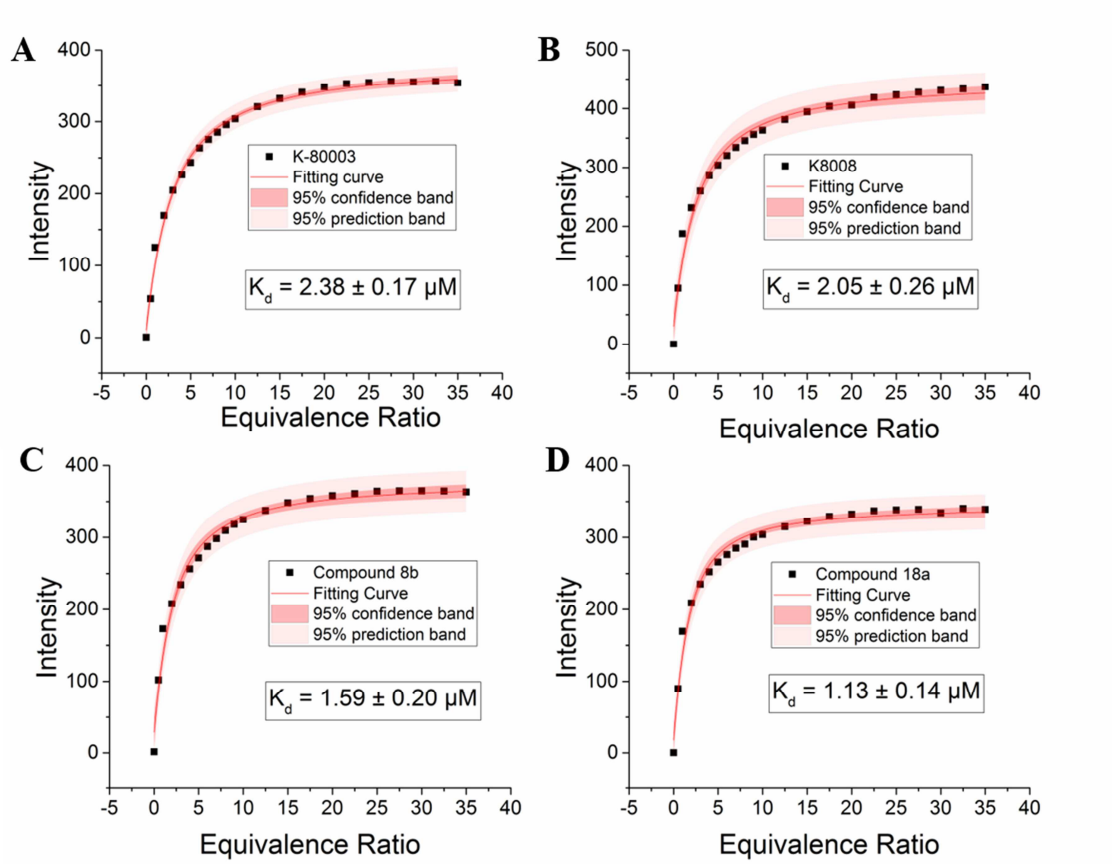

Fig 4. Fluorescence quenching assay. 1 μmol/L protein solution was added in cuvette and compounds with increasing concentration of 0.5 μmol/L to 35 μmol/L was titrated to the cuvette. The excitation wavelength was set at 280 nm and emission was detected from 290 nm to 450 nm. The value of the fluorescence intensity in 300 nm were recorded as F. Y-axis value was set to $F-F_0$ and X-axis value was set to the equivalence ratio of compounds concentration to protein concentration. Four compounds were tested: (A) K-80003 (B) K-8008 (C) compound **8b** (D) compound **18a**.

3.5 K-8008 derivatives induce the cleavage of poly (ADP-ribose) polymerase (PARP)

We further evaluated the apoptotic effect of **8b** and **18a** at protein level and its dependency on RXRα. Firstly, poly (ADP-ribose) polymerase (PARP) cleavage assay showed that both the compounds (**8b** and **18a**) exerted improved PARP cleavage activity in comparison with K-8008

(Fig. 5A and 5C). Furthermore, their PARP cleavage effect was dose-dependent. Previously, we reported that sulindac analogs could inhibit the TNFα-induced AKT activation in cancer cells and enhanced the TNFα -induced apoptosis [19]. Thus, we further tested the PARP cleavage effect of compound **8b** or **18a** in combination with TNFα. Fig. 5B and 5D showed that treatment of HeLa cells or MCF-7 cells with compound **8b** or **18a** in combination with TNFα could significantly enhance the cleavage PARP. Knocking down RXRα expression in HeLa cells by siRNA weakened the effect of compounds **8b** and **18a** on inducing the PARP cleavage (Fig. 6A), implying that the compounds' apoptotic effect is RXRα-dependent. Similar results were observed in MCF-7 cancer cell (Fig. 6B).

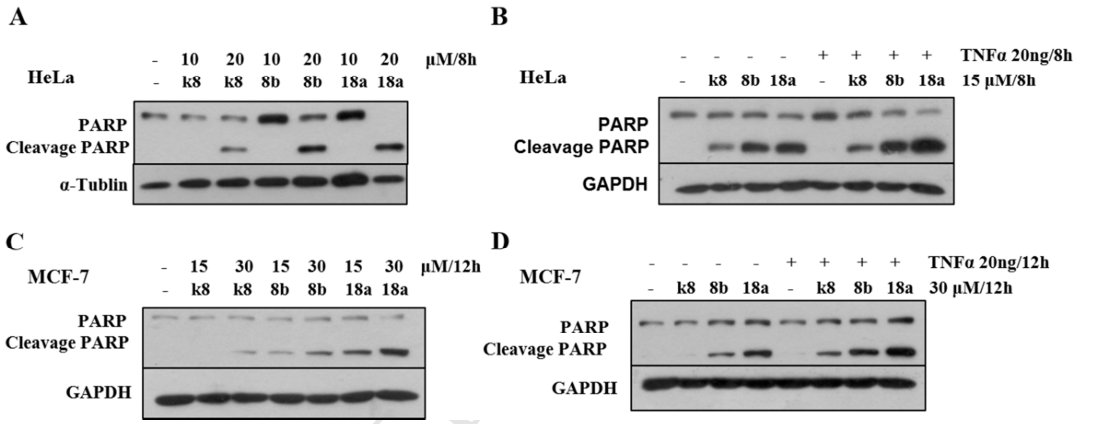

Fig 5. Induction of PARP cleavage by K-8008 (labeled as k8) and its derivatives without (A) or with TNF-α (B) in HeLa Cells and without (C) or with TNF-α (D) in MCF-7 Cells. Cells cultured in medium with 0% FBS were treated with compounds and/or TNF-α (20 ng/mL) for 8 hours in Hela or 12 hours in MCF-7 and analyzed for PARP cleavage by immunoblotting.

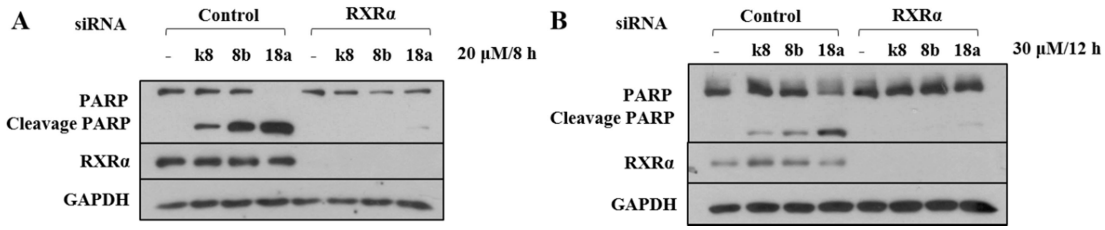

Fig 6. RXRα siRNA transfection inhibits the apoptotic effect of K-8008 (labeled as k8). (A) HeLa cells transfected with control or RXRα siRNA for 48 h were treated with K-8008 and its derivatives **8b** or **18a** (20 μM) for 8 h and analyzed by immunoblotting. (B) MCF-7 cells transfected with control or RXRα siRNA for 48 h were treated with **8b** or **18a** (30 μM) for 12 h and analyzed by immunoblotting.

3.6 Molecular docking studies

Compounds **8b** and **18a** displayed similar binding affinities to RXRα-LBD and comparable biological activities, though they are different structurally. Thus, we were intrigued to understand their binding modes, and therefore perform molecular docking to study their binding conformations.

For compound **8b**, the original goal was to mimic the binding mode of K-8008 while introducing some modification in the R_2 group (Table 1) to enhance its interaction with the protein in the lipophilic tail. Therefore, the K-8008/RXRα-LBD complex crystal structure (PDB code: 4N8R) was used for docking study. The results (Fig. 7A) showed that the binding mode of **8b** was almost identical to K-8008 [20]. Notably, trifluoromethoxy of **8b** was positioned closely to Ala271 and form stronger interaction with Ala 271 compared with K-8008 through its fluorine atoms (Fig. 7B). This may explain why compound **8b** exerts slightly enhanced activity over K-8008.

Compound **18a** was designed based on the bioisostere concept by replacing the carboxylic acid in K-80003 with hydroxyformamide. Thus, the K-80003/RXRα-LBD complex crystal structure (PDB code: 5TBP) was used to carry out the docking study. As 3 K-80003 molecules can bind to the same large hydrophobic cavity where only one K-8008 molecule is bound in the crystal structure of RXRα-LBD/K-80008 complex [23], we assumed that like K-80003 3 **18a** molecules would bind to each large hydrophobic cavity in the RXRα-LBD tetramer, and therefore docked 3 **18a** molecules separately to the three different regions where the 3 K-80003 molecules bind (Fig. 8). In general, **18a** molecules (labeled as **18a-A**, **18a-B** and **18a-C**) bound in a similar fashion to the

K-80003 molecule, especially **18a-A** and **18a-B** (Fig. 8). As K-80003A molecule**, 18a-A** could form hydrogen bond with Trp305 in chain A. However, the π-π interaction between Trp305 and the ligand seems to be stronger for **18a-A** because both of the two benzene rings of **18a-A** could contribute to the π-π interaction whereas only one of the two benzene rings of K-80003A could form π-π interaction with Trp305. **18a-B** was predicted to form hydrogen bond with backbone of Arg302 in chain C, differently from K-80003B which forms a H-bond with Trp305 in chain C. Other than that, **18a-B** and K-80003B make similar hydrophobic interaction with the protein. **18a-C** could make stronger interaction with the protein than K-80003C by forming 4 hydrogen bonds with Gln275, Arg316 and backbones of Ala327 and Leu309 in chain A (Fig. 8). Overall, our docking results showed that **18a** may display an enhanced bind affinity to RXRα -LBD tetramer than K-80003.

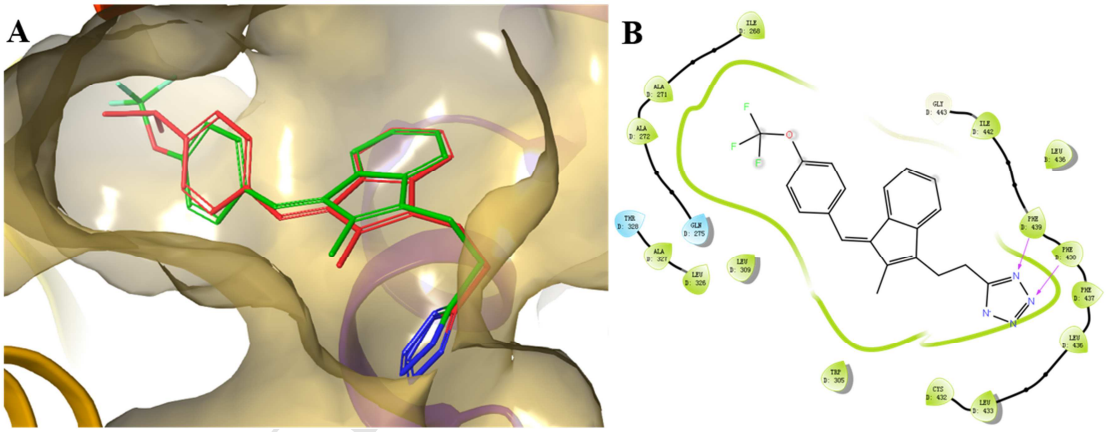

Fig. 7. Molecular docking study of compound **8b**. (A) Compound **8b** was docked to the K-8008/RXRα-LBD complex crystal structure (PDB code: 4N8R) and superimposed with K-8008. Compound **8b** was showed in red sticks and K-8008 in green sticks. The binding pocket of **8b** was showed in yellow surface. (B) The interactions between compound **8b** and RXRα in 2-D drawing.

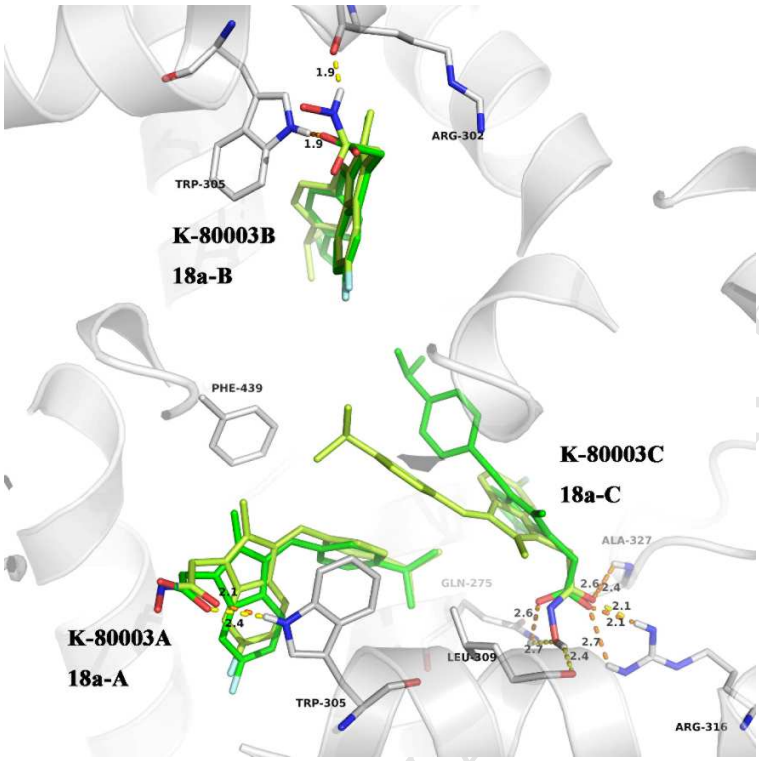

Fig. 8. Molecular docking studies of compound **18a**. Compound **18a** was separately docked to the regions where the three molecules of K-80003 bind in the K-80003/RXRα crystal structure (PDB code: 5TBP). 18a was showed in yellow sticks, K-80003 in green sticks and the amino acid residue in white sticks. The hydrogen bonds between 18a and RXRα were showed in yellow dashed lines and K-80003 and RXRα in orange dashed lines.

4. Conclusion

In summary, we have reported studies on a series of new K-8008 derivatives on their SAR as anticancer agents targeting RXRα. Two new compounds, **8b** and **18a**, showed slightly enhanced anticancer activity compared to K-8008. Compound **8b** was 1.4-fold (IC_{50} = 8.90 ± 0.72 μM) more potent than K-8008 in MDA-MB-231 cancer cell line and 1.6-fold (IC_{50} =17.34 ± 0.78 μM) in MCF-7 and the **18a** compound was 2.5-fold (IC_{50} = 5.00 ± 0.57 μM) more potent than K-8008 in MDA-MB-231 cancer cell line and 1.3-fold (IC_{50} = 20.77 ± 0.78 μM) in MCF-7. The dissociation constant (K_d) of **8b** and **18a** was 1.59 ± 0.20 μM and 1.13 ± 0.14 μM, respectively. Further

biological evaluation revealed that **8b** and **18a** are more potent than K-8008 in inducing PARP cleavage and the apoptotic effects of the compounds are RXRα-dependent. The studies also demonstrated the feasibility of replacing the polar group in K-8008 with different carboxyl bioisosteres as an optimization approach.

5. Experiment section

5.1 Chemistry

5.1.1 General procedure A: the synthesis of indene derivative from appropriate indene moiety.

To a solution of corresponding indene products (0.25 mmol, 1.0 equiv) in MeOH (5.0 mL) was added 2.5 N NaOMe (0.75 mmol, 0.25 mL, 3.0 equiv) at room temperature to get an orange mixture. After stirring for 30 min, the mixture was added with appropriate aromatic aldehyde (0.5 mmol, 2 equiv). The resulting mixture was refluxed at 80 °C for 4 h. After concentrated under reduced pressure, the residue was acidified with a 1 N HCl solution to pH 4.0~6.0. After stirring for another 0.5 h at room temperature, the mixture was extracted with EtOAc (15 mL *3). The combined organic layers were dried over anhydrous Na_2SO_4, filtered, and concentrated under reduced pressure. The residue was purified by flash chromatography to afford indene derivative [21].

5.1.2 Compound **1-6a**.

Compound 1-6a was synthesized according to the reference [19, 20].

5.1.3 Compound **7a**.

Compound **7a** was synthesized according to the reference [20, 21].

5.1.4 (Z)-5-(2-(2-methyl-1-(naphthalen-1-ylmethylene)-1H-inden-3-yl)ethyl)-1H-tetrazol (**8a**)

Compound **8a** was synthesized according to the general procedure A. Yellow solid, 74 mg, yield: 81.7%. ^{1}H NMR (600 MHz, DMSO-d_6) δ 8.03 (t, *J* = 7.06 Hz, 2H), 7.96 (d, *J* = 8.25 Hz, 1H),

7.65 (s, 1H), 7.63 (d, *J* = 6.97 Hz, 1H), 7.61 (d, *J* = 7.89 Hz, 1H), 7.58 (d, *J* = 8.07 Hz, 1H), 7.54 (t, *J* = 7.50 Hz, 1H), 7.23 (d, *J* = 7.52 Hz, 1H), 7.12 (t, *J* = 7.34 Hz, 1H), 6.73 (t, *J* = 7.43 Hz, 1H), 6.66 (d, *J* = 7.52 Hz, 1H), 3.15 (t, *J* = 7.61 Hz, 2H), 3.03 (t, *J* = 7.52 Hz, 2H), 2.12 (s, 3H); ^{13}C NMR (151 MHz, DMSO-d_6) δ 144.2, 142.8, 137.7, 134.8, 134.6, 134.3, 133.7, 131.4, 129.0, 128.9, 128.5, 128.3, 127.4, 127.0, 126.8, 126.0, 125.4, 124.7, 122.7, 118.3, 23.9, 22.7, 10.2. HRMS (ESI) calcd for $C_{24}H_{19}N_4$ $[M-H]^-$: 363.1610; found: 363.1614.

5.1.5 (Z)-5-(2-(2-methyl-1-(4-(trifluoromethoxy)benzylidene)-1H-inden-3-yl)ethyl)-1H-tetrazole (**8b**)

Compound **8b** was synthesized according to the general procedure A. Yellow solid, 94 mg, yield: 94.7%. ^{1}H NMR (600 MHz, DMSO-d_6) δ 7.65 (dd, *J* = 1.00, 8.44 Hz, 2H), 7.46 (d, *J* = 8.07 Hz, 2H), 7.23 - 7.26 (m, 2H), 7.16 - 7.21 (m, 2H), 6.92 (t, *J* = 7.90 Hz, 1H), 3.11 (t, *J* = 7.61 Hz, 2H), 2.99 (t, *J* = 7.52 Hz, 2H), 1.97 (s, 3H); ^{13}C NMR (151 MHz, DMSO-d_6) δ 148.4, 144.3, 141.8, 137.8, 136.2, 134.9, 134.1, 131.6, 129.1, 128.6, 125.0, 122.4, 121.5, 119.72, 118.4, 23.9, 22.6, 10.1. HRMS (ESI) calcd for $C_{21}H_{16}F_3N_4O$ $[M-H]^-$: 397.1276; found: 397.1278.

5.1.6 (Z)-5-(2-(1-(4-(tert-butyl)benzylidene)-2-methyl-1H-inden-3-yl)ethyl)-1H-tetrazole (**8c**)

Compound **8c** was synthesized according to the general procedure A. Yellow solid, 63 mg, yield: 68.5%. ^{1}H NMR (600 MHz, CHLOROFORM-d) δ 7.47 (d, *J* = 7.52 Hz, 1H), 7.38 - 7.42 (m, 4H), 7.10 (dd, *J* = 1.00, 7.30 Hz, 1H), 7.09 (d, *J* = 7.15 Hz, 1H), 7.07 (s, 1H), 6.88 (dt, *J* = 1.00, 7.30 Hz, 1H), 3.27 (t, *J* = 7.52 Hz, 2H), 3.05 (t, *J* = 7.61 Hz, 2H), 1.92 (s, 3H), 1.36 (s, 9H); ^{13}C NMR (151 MHz, CHLOROFORM-d) δ 151.4, 143.5, 140.6, 135.7, 135.6, 134.4, 133.6, 130.8, 129.2, 127.8, 125.3, 124.6, 122.9, 117.4, 34.8, 31.3, 24.0, 22.6, 10.0. HRMS (ESI) calcd for $C_{24}H_{25}N_4$ $[M-H]^-$: 369.2079; found: 369.2079.

5.1.7 (Z)-5-(2-(1-(4-methoxybenzylidene)-2-methyl-1H-inden-3-yl)ethyl)-1H-tetrazole (**8d**)

Compound **8d** was synthesized according to the general procedure A. Yellow solid, 36.29 mg, yield: 42.2%. ^{1}H NMR (600 MHz, DMSO-d_6) δ 7.50 (d, *J* = 8.62 Hz, 2H), 7.43 (d, *J* = 7.52 Hz, 1H), 7.24 (d, *J* = 7.34 Hz, 1H), 7.20 (s, 1H), 7.18 (dt, *J* = 1.00, 7.50 Hz, 1H), 7.04 (d, *J* = 8.62 Hz, 2H), 6.93 (dt, *J* = 1.01, 7.47 Hz, 1H), 3.83 (s, 3H), 3.11 (t, *J* = 7.61 Hz, 2H), 2.99 (t, *J* = 7.61 Hz, 2H), 1.97 (s, 3H); ^{13}C NMR (151 MHz, DMSO-d_6) δ 159.8, 144.1, 140.0, 136.6, 135.1, 134.3, 131.4, 130.9, 128.9, 128.1, 124.7, 122.3, 118.2, 114.4, 55.7, 23.9, 22.8, 10.2. HRMS (ESI) calcd for $C_{21}H_{19}N_4O$ [M-H]$^-$: 343.1559; found: 343.1561.

5.1.8 (Z)-5-(2-(2-methyl-1-(4-(methylthio)benzylidene)-1H-inden-3-yl)ethyl)-1H-tetrazole (**8e**)

Compound **8e** was synthesized according to the general procedure A. Yellow solid, 46 mg, yield: 51.5%. ^{1}H NMR (600 MHz, DMSO-d_6) δ 7.49 (d, *J* = 8.07 Hz, 2H), 7.39 (d, *J* = 7.70 Hz, 1H), 7.35 (d, *J* = 7.89 Hz, 2H), 7.24 (d, *J* = 7.34 Hz, 1H), 7.20 (s, 1H), 7.17 (dt, *J* = 1.00, 7.20 Hz, 1H), 6.93 (dt, *J* = 1.00, 8.10 Hz, 1H), 3.11 (t, *J* = 7.61 Hz, 2H), 2.99 (t, *J* = 7.61 Hz, 2H), 2.54 (s, 3H), 1.97 (s, 3H); ^{13}C NMR (151 MHz, DMSO-d_6) δ 144.2, 140.7, 139.3, 137.1, 135.1, 134.2, 133.0, 130.4, 130.4, 128.3, 125.9, 124.8, 122.5, 118.3, 23.9, 22.7, 14.8, 10.2. HRMS (ESI) calcd for $C_{21}H_{19}N_4S$ [M-H]$^-$: 359.1331; found: 359.1334.

5.1.9 (Z)-5-(2-(1-(2-chlorobenzylidene)-2-methyl-1H-inden-3-yl)ethyl)-1H-tetrazole (**8f**)

Compound **8f** was synthesized according to the general procedure A. Yellow solid, 60 mg, yield: 69.3%. ^{1}H NMR (600 MHz, DMSO-d_6) δ 7.62 (dd, *J* = 1.00, 8.44 Hz, 1H), 7.57 (dd, *J* = 1.19, 7.43 Hz, 1H), 7.47 (dt, *J* = 1.56, 7.66 Hz, 1H), 7.44 (dt, *J* = 1.19, 7.47 Hz, 1H), 7.25 (d, *J* = 7.52 Hz, 1H), 7.19 (dt, *J* = 1.00, 6.40 Hz, 1H), 7.14 (s, 1H), 6.89 (t, *J* = 7.89 Hz, 2H), 3.15 (t, *J* = 7.61 Hz, 2H), 3.01 (t, *J* = 7.61 Hz, 2H), 2.01 (s, 3H); ^{13}C NMR (151 MHz, DMSO-d_6) δ 144.2, 142.4, 138.3, 135.3, 134.5, 134.2, 133.0, 131.7, 130.6, 130.0, 128.7, 127.6, 126.8, 125.0, 122.5, 118.5, 23.8, 22.5, 10.1. HRMS (ESI) calcd for $C_{20}H_{16}ClN_4$ [M-H]$^-$: 347.1064; found: 347.1066.

5.1.10 (Z)-5-(2-(1-(3-chlorobenzylidene)-2-methyl-1H-inden-3-yl)ethyl)-1H-tetrazole (**8g**)

Compound **8g** was synthesized according to the general procedure A. Yellow solid, 79 mg, yield: 90.7%. ^{1}H NMR (600 MHz, DMSO-d_6) δ 7.52 (s, 1H), 7.48 (d, *J* = 7.15 Hz, 1H), 7.44 - 7.47 (m, 2H), 7.23 (d, *J* = 7.34 Hz, 1H), 7.14 - 7.20 (m, 3H), 6.90 (dt, *J* = 1.00, 7.90 Hz, 1H), 3.12 (t, *J* = 7.52 Hz, 2H), 2.99 (t, *J* = 7.61 Hz, 2H), 1.95 (s, 3H); ^{13}C NMR (151 MHz, DMSO-d_6) δ 144.3, 142.1, 139.1, 138.0, 134.9, 134.1, 133.7, 130.8, 129.1, 128.9, 128.6, 128.4, 128.2, 125.0, 122.5, 118.5, 23.8, 22.6, 10.1. HRMS (ESI) calcd for $C_{20}H_{16}ClN_4$ [M-H]$^-$: 347.1064; found: 347.1066.

5.1.11 (Z)-5-(2-(1-(4-chlorobenzylidene)-2-methyl-1H-inden-3-yl)ethyl)-1H-tetrazole (**8h**)

Compound **8h** was synthesized according to the general procedure A. Yellow solid, 55 mg, yield: 63.7%. ^{1}H NMR (600 MHz, DMSO-d_6) δ 7.49 - 7.55 (m, 4H), 7.23 (t, *J* = 8.30 Hz, 2H), 7.15 - 7.20 (m, 2H), 6.91 (t, *J* = 7.43 Hz, 1H), 3.11 (t, *J* = 7.52 Hz, 2H), 2.99 (t, *J* = 7.52 Hz, 2H), 1.96 (s, 3H); ^{13}C NMR (151 MHz, DMSO-d_6) δ 155.9, 144.2, 141.7, 137.7, 135.7, 135.0, 134.1, 133.3, 131.5, 129.3, 129.0, 128.5, 124.9, 122.5, 118.4, 23.9, 22.6, 10.1. HRMS (ESI) calcd for $C_{20}H_{16}ClN_4$ [M-H]$^-$: 347.1064; found: 347.1066.

5.1.12 (Z)-5-(2-(2-methyl-1-(2-(trifluoromethyl)benzylidene)-1H-inden-3-yl)ethyl)-1H-tetrazole (**8i**)

Compound **8i** was synthesized according to the general procedure A. Yellow solid, 56 mg, yield: 58.5%. ^{1}H NMR (600 MHz, DMSO-d_6) δ 7.89 (d, *J* = 7.89 Hz, 1H), 7.75 (t, *J* = 7.43 Hz, 1H), 7.67 (t, *J* = 7.70 Hz, 1H), 7.59 (d, *J* = 7.52 Hz, 1H), 7.28 (d, *J* = 1.00 Hz, 1H), 7.25 (d, *J* = 7.34 Hz, 1H), 7.17 (dt, *J* = 1.00, 8.10 Hz, 1H), 6.83 (dt, *J* = 1.00, 7.90 Hz, 1H), 6.49 (d, *J* = 7.70 Hz, 1H), 3.13 (t, *J* = 7.70 Hz, 2H), 3.00 (t, *J* = 7.70 Hz, 2H), 2.00 (s, 3H); ^{13}C NMR (151 MHz, DMSO-d_6) δ 144.2, 142.9, 138.6, 135.9, 134.3, 134.2, 133.1, 131.8, 129.2, 128.6, 127.43, 126.6, 126.0, 125.0, 124.59, 122.6, 118.6, 23.8, 22.5, 10.0. HRMS (ESI) calcd for $C_{21}H_{16}F_3N_4$ [M-H]$^-$: 381.1327; found: 381.1329.

5.1.13 (Z)-5-(2-(2-methyl-1-(3-(trifluoromethyl)benzylidene)-1H-inden-3-yl)ethyl)-1H-tetrazole (**8j**)

Compound **8j** was synthesized according to the general procedure A. Yellow solid, 39 mg, yield: 40.8%. ^{1}H NMR (600 MHz, DMSO-d_6) δ 7.85 (d, *J* = 6.42 Hz, 2H), 7.78 (d, *J* = 7.70 Hz, 1H), 7.72 (t, *J* = 7.98 Hz, 1H), 7.31 (s, 1H), 7.27 (d, *J* = 7.34 Hz, 1H), 7.20 (dt, *J* = 1.00, 7.90 Hz, 1H), 7.11 (d, *J* = 7.70 Hz, 1H), 6.91 (dt, *J* = 1.00, 7.90 Hz, 1H), 3.13 (t, *J* = 7.61 Hz, 2H), 3.01 (t, *J* = 7.61 Hz, 2H), 1.98 (s, 3H); ^{13}C NMR (151 MHz, DMSO-d_6) δ 144.4, 142.3, 138.1, 138.0, 135.0, 134.0, 133.6, 130.1, 129.8, 128.8, 128.8, 126.2, 125.1, 125.0, 124.6, 122.2, 118.6, 23.9, 22.6, 10.1. HRMS (ESI) calcd for $C_{21}H_{16}F_3N_4$ $[M-H]^-$: 381.1327; found: 381.1328.

5.1.14 (Z)-5-(2-(2-methyl-1-(4-(trifluoromethyl)benzylidene)-1H-inden-3-yl)ethyl)-1H-tetrazole (**8k**)

Compound **8k** was synthesized according to the general procedure A. Yellow solid, 57 mg, yield: 60%. ^{1}H NMR (600 MHz, DMSO-d_6) δ 7.84 (d, *J* = 8.25 Hz, 2H), 7.74 (d, *J* = 8.07 Hz, 2H), 7.28 (s, 1H), 7.26 (d, *J* = 7.34 Hz, 1H), 7.20 (t, *J* = 7.43 Hz, 1H), 7.15 (d, *J* = 7.52 Hz, 1H), 6.93 (t, *J* = 7.34 Hz, 1H), 3.13 (t, *J* = 7.52 Hz, 2H), 3.01 (t, *J* = 7.61 Hz, 2H), 1.98 (s, 3H); ^{13}C NMR (151 MHz, DMSO-d_6) δ 144.3, 142.4, 141.3, 138.3, 134.9, 134.0, 130.4, 128.8, 125.9, 125.8, 125.8, 125.1, 124.7, 122.5, 118.5, 23.9, 22.6, 10.1. HRMS (ESI) calcd for $C_{21}H_{16}F_3N_4$ $[M-H]^-$: 381.1327; found: 381.1329.

5.1.15 (E)-5-(2-(1-(4-isopropylbenzylidene)-1H-inden-3-yl)ethyl)-1H-tetrazole (**9a**)

Compound **9a** was synthesized according to the general procedure A. Yellow solid, 70 mg, yield: 84.0%. ^{1}H NMR (600 MHz, DMSO-d_6) δ 7.81 (d, *J* = 7.15 Hz, 1H), 7.60 (d, *J* = 8.25 Hz, 2H), 7.55 (s, 1H), 7.38 (d, *J* = 7.34 Hz, 1H), 7.35 (d, *J* = 8.07 Hz, 2H), 7.29 (dt, *J* = 1.10, 7.34 Hz, 1H), 7.26 (dt, *J* = 0.92, 7.70 Hz, 1H), 6.89 (s, 1H), 3.35 (t, *J* = 8.10 Hz, 2H), 3.11 (t, *J* = 7.52 Hz, 2H),

2.94 (quind, *J* = 6.87, 13.80 Hz, 1H), 1.24 (d, *J* = 6.79 Hz, 6H); ^{13}C NMR (151 MHz, DMSO-d_6) δ 149.5, 146.6, 141.5, 138.5, 137.9, 134.6, 130.7, 128.0, 127.7, 127.4, 125.9, 122.1, 119.8, 119.2, 33.7, 25.7, 24.2, 22.1. HRMS (ESI) calcd for $C_{22}H_{21}N_4$ $[M-H]^-$: 341.1766; found: 341.1767.

5.1.16 2-(2-methyl-1H-inden-3-yl)acetonitrile (**10a**)

Diethyl cyanomethylphosphonate (13.409 g, 2 equiv) was dissolved in 65 mL acetonitrile in 0 °C, and was dropwise added with DBU (17.272 g, 3 equiv), stirring for 30 min. The mixture was added with compound 4a (5 g, 1 equiv) and stirred at room temperature overnight. After concentrated under reduced pressure, the mixture was extracted with EtOAc (15 mL *3) and washed with brine (15 mL). The combined organic layers were dried over anhydrous Na_2SO_4, filtered, and concentrated under reduced pressure. The residue was purified by flash chromatography to afford compound **10a**. White solid, 3.5 g, yield : 75%. ^{1}H NMR (600 MHz, CHLOROFORM-d) δ 7.39 (d, *J* = 7.34 Hz, 1H), 7.32 (d, *J* = 7.15 Hz, 1H), 7.31 (t, *J* = 7.52 Hz, 1H), 7.18 (dt, *J* = 1.19, 7.20 Hz, 1H), 3.54 (s, 2H), 3.35 (s, 2H), 2.15 (s, 3H); ^{13}C NMR (151 MHz, CHLOROFORM-d) δ 144.1, 143.2, 141.8, 126.6, 125.5, 124.8, 123.5, 118.0, 117.1, 42.9, 14.2, 13.9. HRMS (ESI) calcd for $C_{12}H_{11}NNa^+$ $[M+Na]^+$: 192.0789; found: 192.0784.

5.1.17 2-(1H-inden-3-yl)acetonitrile (**10b**)

Compound **10b** was synthesized according to compound **10a**. White solid, 4.3 g, yield: 60%. ^{1}H NMR (600 MHz, CHLOROFORM-d) δ 7.53 (d, *J* = 7.89 Hz, 1H), 7.40 (t, *J* = 7.24 Hz, 1H), 7.37 (d, *J* = 7.34 Hz, 1H), 7.28 (t, *J* = 7.50 Hz, 1H), 5.65 (s, 1H), 3.08 - 3.13 (m, 4H); ^{13}C NMR (151 MHz, CHLOROFORM-d) δ 167.4, 149.7, 138.1, 131.8, 127.2, 125.9, 121.6, 118.3, 85.8, 31.4, 29.9. HRMS (ESI) calcd for $C_{11}H_9NNa^+$ $[M+Na]^+$: 178.0633; found: 178.0628.

5.1.18 N-hydroxy-2-(2-methyl-1H-inden-3-yl)acetimidamide (**11**)

To a solution of compound **10a** (338 mg, 1 equiv) was dissolved in EtOH (5 mL) and was added with hydroxylamine of 50% w.t. in water (528 mg, 8 equiv) at 80 °C for 3 h. The mixture was extracted with EtOAc (30 mL *3) and washed with brine (30 mL *3). The combined organic layers were dried over anhydrous Na_2SO_4, filtered, and concentrated under reduced pressure. The residue was purified by flash chroma- tography to afford indene derivative. White solid, 363 mg, yield: 92%.^{1}H NMR (600 MHz, DMSO-d_6) δ 8.90 (s, 1H), 7.34 (t, *J* = 6.60 Hz, 2H), 7.17 (t, *J* = 7.70 Hz, 1H), 7.06 (dt, *J* = 1.00, 7.70 Hz, 1H), 5.18 (s, 2H), 3.28 (s, 2H), 3.22 (s, 2H), 2.09 (s, 3H); ^{13}C NMR (151 MHz, DMSO-d_6) δ 151.3, 146.8, 142.3, 141.2, 132.2, 126.2, 123.9, 123.3, 119.2, 42.6, 27.8, 14.4. HRMS (ESI) calcd for $C_{12}H_{13}N_2O$ $[M-H]^-$: 201.1028; found: 201.1024.

5.1.19 3-((2-methyl-1H-inden-3-yl)methyl)-1,2,4-oxadiazol-5(4H)-one (**12**)

Compound **11** (404 mg, 1 equiv) in 6 mL dioxane was added with CDI (389 mg, 1.2 equiv) and DBU (334 mg, 1.1 equiv). After stirring at 100 °C for 4 h, the residue was acidified with a 1 N HCl solution to pH 4.0~6.0. After stirring for another 0.5 h at room temperature, the mixture was extracted with EtOAc (30 mL *3). The combined organic layers were dried over anhydrous Na_2SO_4, filtered, and concentrated under reduced pressure. The residue was purified by flash chroma- tography to afford product **12**. White solid, 242 mg, yield: 53%. ^{1}H NMR (600 MHz, DMSO-d_6) δ 7.39 (d, *J* = 7.34 Hz, 1H), 7.20 - 7.25 (m, 2H), 7.11 (dt, *J* = 2.20, 7.00 Hz, 1H), 3.80 (s, 2H), 3.36 (s, 2H), 2.12 (s, 3H). ^{13}C NMR (151 MHz, DMSO-d_6) δ 160.4, 158.8, 145.5, 144.1, 142.3, 128.4, 126.5, 124.4, 123.7, 118.6, 42.8, 21.7, 14.5. HRMS (ESI) calcd for $C_{13}H_{12}N_2O_2Na^+$ $[M+Na]^+$: 251.0797; found: 251.0791.

5.1.20

(Z)-3-((1-(4-isopropylbenzylidene)-2-methyl-1H-inden-3-yl)methyl)-1,2,4-oxadiazol-5(4H)-one (**13a**)

Compound **13a** was synthesized according to the general procedure A. Yellow solid, 48 mg, yield: 54%. ^{1}H NMR (600 MHz, DMSO-d_6) δ 12.35 (br.s., 1H), 7.50 (d, *J* = 7.89 Hz, 2H), 7.42 (d, *J* = 7.70 Hz, 1H), 7.33 - 7.39 (m, 3H), 7.20 (d, *J* = 7.15 Hz, 1H), 7.17 (t, *J* = 7.06 Hz, 1H), 6.93 (dt, *J* = 0.92, 7.90 Hz, 1H), 3.89 (s, 2H), 2.96 (spt, *J* = 6.88 Hz, 1H), 2.20 (s, 3H), 1.25 (d, *J* = 6.79 Hz, 6H); ^{13}C NMR (151 MHz, DMSO-d_6) δ 160.3, 158.6, 149.4, 143.8, 140.2, 137.8, 134.0, 134.0, 132.3, 130.3, 129.9, 128.3, 126.9, 125.0, 122.4, 118.6, 33.8, 24.2, 22.0, 10.8. HRMS (ESI) calcd for $C_{23}H_{22}N_2O_2Na^+$ $[M+Na]^+$: 381.1579; found: 381.1574.

5.1.21 Compound **14-16**

Compound **14-16** was synthesized according to the reference [19].

5.1.22

(Z)-2-(1-(4-isopropylbenzylidene)-2-methyl-1H-inden-3-yl)-N-(1H-tetrazol-5-yl)acetamide (**17a**)

To a solution of **16** (141 mg, 1 equiv.) was added HOBT (72 mg, 1.2 equiv.) and EDCI (101 mg, 1.2 equiv.) at 0 °C for 1 h. Then, amino-1H-tetrazole (85 mg, 2.5 equiv.) was added to the mixture and stirring in room temperature for 12 h. The mixture was extracted with EtOAc (30 mL *3). The combined organic layers were dried over anhydrous Na_2SO_4, filtered, and concentrated under reduced pressure. The residue was purified by flash chroma- tography to afford product **17a**. Yellow solid, 88 mg, yield: 87%. ^{1}H NMR (600 MHz, DMSO-d_6) δ 15.87 (br. s., 1H), 12.33 (br. s., 1H), 7.49 (d, *J* = 8.07 Hz, 2H), 7.35 - 7.38 (m, 3H), 7.34 (s, 1H), 7.19 (dd, *J* = 2.38, 9.35 Hz, 1H), 6.75 (dt, *J* = 2.38, 8.80 Hz, 1H), 3.83 (s, 2H), 2.96 (spt, *J* = 6.88 Hz, 1H), 2.22 (s, 3H), 1.26 (d, *J* = 6.79 Hz, 6H); ^{13}C NMR (151 MHz, DMSO-d_6) δ 169.2, 162.8, 149.4, 147.2, 139.4, 139.3, 133.8, 131.9, 131.6, 130.0, 129.9, 127.0, 123.5, 110.8, 106.6, 33.8, 32.6, 24.2, 11.0. HRMS (ESI) calcd for $C_{23}H_{22}FN_5ONa^+$ $[M+Na]^+$: 426.1706; found: 426.1695.

5.1.23 (Z)-N-hydroxy-2-(1-(4-isopropylbenzylidene)-2-methyl-1H-inden-3-yl)acetamide (**18a**)

To a solution of **16** (100 mg, 0.3 equiv) in EtOH (4 mL) was added with H_2SO_4 (0.3 mL) at 60 ℃ for 2 h. The mixture was extracted with EtOAc (30 mL *3). The combined organic layers were dried over anhydrous Na_2SO_4, filtered, and concentrated under reduced pressure. Without further purification, the products continued to react with hydroxylamine (330 mg, 1.0 equiv) and sodium methoxide (1.0 mL, 2.4 mol/L) in MeOH (5 mL) at room temperature for 4 h. The mixture was extracted with EtOAc (30 mL *3). The combined organic layers were dried over anhydrous Na_2SO_4, filtered, and concentrated under reduced pressure. The residue was purified by flash chroma- tography to afford product **18a**. Yellow solid, 63 mg, yield: 60%. ^{1}H NMR (600 MHz, DMSO-d_6) δ 10.71 (d, *J* = 1.46 Hz, 1H), 8.87 (d, *J* = 1.47 Hz, 1H), 7.46 - 7.50 (m, *J* = 8.07 Hz, 2H), 7.35 - 7.38 (m, *J* = 8.25 Hz, 2H), 7.33 (dd, *J* = 5.32, 8.44 Hz, 1H), 7.29 (s, 1H), 7.13 (dd, *J* = 2.38, 9.35 Hz, 1H), 6.73 (dt, *J* = 2.75, 9.20 Hz, 1H), 3.31 (s, 2H), 2.96 (spt, *J* = 6.88 Hz, 1H), 2.19 (s, 3H), 1.26 (d, *J* = 6.97 Hz, 6H); ^{13}C NMR (151 MHz, DMSO-d_6) δ 166.4, 162.7, 149.3, 147.4, 139.5, 138.6, 134.0, 132.7, 131.3, 130.1, 129.8, 127.0, 123.4, 110.6, 106.5, 33.8, 30.4, 24.2, 10.9. HRMS (ESI) calcd for $C_{22}H_{22}FNO_2Na^+$ $[M+Na]^+$: 374.1533; found: 374.1526.

5.1.24 5-((2-methyl-1H-inden-3-yl)methyl)-1H-tetrazole (**19a**)

A flask (10 mL) was charged with compound 10a (310 mg, 2 mmol), dry DMF (8 mL), triethylamine hydrochloride (1.1 g, 8 mmol) and sodium azide (520 mg, 8 mmol) which were added to the solution under nitrogen. The mixture was heated for 40 h at 110 ℃, then cooled to the room temperature, concentrated in vacuo and diluted with water (100 mL). The aqueous solution was then acidified to pH 2.0 using concentrated HCl, extracted with EtOAc (30 mL*3). The combined organic layers were washed with brine(30 mL), dried over anhydrous Na_2SO_4, filtered, and concentrated under reduced pressure. The residue was purified by flash chromatography (ethyl acetate : PE = 1 : 1) to afford crude compound **19a**. White solid, 299 mg, yield : 77%. ^{1}H NMR (600 MHz, DMSO-d_6) δ 7.37 (d, *J* = 7.34 Hz, 1H), 7.17 (t, *J* = 7.24 Hz, 1H), 7.14 (d, *J* = 7.15 Hz, 1H), 7.09 (dt, *J* = 1.00, 7.30 Hz, 1H), 4.17 (s, 2H), 3.36 (s, 2H), 2.13 (s, 3H); ^{13}C NMR (151 MHz,

DMSO-d_6) δ 145.6, 142.8, 142.5, 130.7, 126.4, 124.3, 123.7, 118.6, 42.7, 19.9, 14.4. HRMS (ESI) calcd for $C_{12}H_{11}N_4$ $[M-H]^-$: 211.0984; found: 211.0979.

5.1.25 5-((1H-inden-3-yl)methyl)-1H-tetrazole (**19b**)

Compound 19b was synthesized using the same method of **19a**. White solid, 222 mg, yield : 56%. ^{1}H NMR (600 MHz, DMSO-d_6) δ 7.49 (d, *J* = 7.34 Hz, 1H), 7.34 (d, *J* = 7.34 Hz, 1H), 7.27 (t, *J* = 7.34 Hz, 1H), 7.21 (t, *J* = 7.30 Hz, 1H), 6.34 (s, 1H), 4.25 (d, *J* = 1.47 Hz, 2H), 3.38 (s, 2H); ^{13}C NMR (151 MHz, DMSO-d_6) δ 144.4, 144.2, 138.4, 132.0, 126.5, 125.4, 124.3, 119.5, 37.9, 22.6. HRMS (ESI) calcd for $C_{11}H_9N_4$ $[M-H]^-$: 197.0827; found: 197.0822.

5.1.26 (Z)-5-((1-(4-isopropylbenzylidene)-2-methyl-1H-inden-3-yl)methyl)-1H-tetrazole (**20a**)

Compound **20a** was synthesized according to the general procedure A. Yellow solid, 25 mg, yield: 29.1 %. ^{1}H NMR (600 MHz, DMSO-d_6) δ 7.50 (d, *J* = 7.89 Hz, 2H), 7.40 (d, *J* = 7.52 Hz, 1H), 7.37 (s, 1H), 7.35 (d, *J* = 3.48 Hz, 2H), 7.13 (t, *J* = 7.20 Hz, 1H), 7.10 (d, *J* = 7.15 Hz, 1H), 6.92 (dt, *J* = 1.10, 7.90 Hz, 1H), 4.25 (s, 2H), 2.96 (spt, *J* = 7.00 Hz, 1H), 2.22 (s, 3H), 1.26 (d, *J* = 6.97 Hz, 6H); ^{13}C NMR (151 MHz, CHLOROFORM-d) δ 149.5, 143.0, 140.2, 137.4, 134.1, 133.7, 132.1, 129.5, 128.0, 126.6, 125.0, 123.0, 117.7, 58.6, 34.0, 23.9, 18.3, 10.5. HRMS (ESI) calcd for $C_{21}H_{19}N_4$ $[M-H]^-$: 341.1766; found: 341.1766.

5.1.27

(Z)-5-((2-methyl-1-(4-(trifluoromethoxy)benzylidene)-1H-inden-3-yl)methyl)-1H-tetrazole (**20b**)

Compound **20b** was synthesized according to the general procedure A. Yellow solid, 52 mg, yield: 54.3%. ^{1}H NMR (600 MHz, DMSO-d_6) δ 7.67 (d, *J* = 8.25 Hz, 2H), 7.49 (d, *J* = 8.44 Hz, 2H), 7.38 (s, 1H), 7.20 (d, *J* = 7.52 Hz, 1H), 7.15 (dt, *J* = 1.00, 7.20 Hz, 1H), 7.12 (d, *J* = 6.79 Hz, 1H), 6.92 (dt, *J* = 1.28, 7.34 Hz, 1H), 4.26 (s, 2H), 2.23 (s, 3H); ^{13}C NMR (151 MHz, DMSO-d_6) δ 148.5,

144.0, 141.6, 136.6, 136.0, 133.8, 133.5, 131.6, 130.2, 128.6, 125.2, 122.4, 121.5, 120.6, 118.8, 20.1, 10.7. HRMS (ESI) calcd for $C_{20}H_{14}F_3N_4O$ $[M-H]^-$: 383.1120; found: 383.1121.

5.1.28 (Z)-5-((1-(4-methoxybenzylidene)-2-methyl-1H-inden-3-yl)methyl)-1H-tetrazole (**20c**)

Compound **20c** was synthesized according to the general procedure A. Yellow solid, 46 mg, yield: 50.6%. ^{1}H NMR (600 MHz, DMSO-d_6) δ 7.53 (d, *J* = 8.62 Hz, 2H), 7.45 (d, *J* = 7.52 Hz, 1H), 7.34 (s, 1H), 7.10 - 7.15 (m, 2H), 7.06 (d, *J* = 8.44 Hz, 2H), 6.93 (dt, *J* = 1.00, 7.20 Hz, 1H), 4.26 (s, 2H), 3.83 (s, 3H), 2.23 (s, 3H); ^{13}C NMR (151 MHz, DMSO-d_6) δ 159.9, 143.8, 139.7, 136.8, 134.1, 132.2, 132.0, 131.5, 128.7, 128.0, 124.9, 122.3, 118.6, 114.5, 55.7, 20.1, 10.8. HRMS (ESI) calcd for $C_{19}H_{15}N_4O$ $[M-H]^-$: 329.1403; found: 329.1404.

5.1.29 (Z)-5-((2-methyl-1-(4-(methylthio)benzylidene)-1H-inden-3-yl)methyl)-1H-tetrazole (**20d**)

Compound **20d** was synthesized according to the general procedure A. Yellow solid, 29 mg, yield: 34.6%. ^{1}H NMR (600 MHz, DMSO-d_6) δ 7.52 (d, *J* = 8.25 Hz, 2H), 7.42 (d, *J* = 7.52 Hz, 1H), 7.36 (d, *J* = 8.25 Hz, 2H), 7.34 (s, 1H), 7.14 (t, *J* = 7.00 Hz, 1H), 7.11 (d, *J* = 6.97 Hz, 1H), 6.93 (dt, *J* = 1.00, 7.70 Hz, 1H), 4.26 (s, 2H), 2.54 (s, 3H), 2.23 (s, 3H); ^{13}C NMR (151 MHz, DMSO-d_6) δ 143.8, 140.5, 139.5, 136.8, 134.0, 132.8, 132.7, 131.5, 130.4, 128.2, 125.9, 125.0, 122.4, 118.6, 20.1, 14.8, 10.7. HRMS (ESI) calcd for $C_{19}H_{15}N_4S$ $[M-H]^-$: 345.1174; found: 345.1175.

5.1.30 (Z)-5-((1-(4-(tert-butyl)benzylidene)-2-methyl-1H-inden-3-yl)methyl)-1H-tetrazole (**20e**)

Compound **20e** was synthesized according to the general procedure A. Yellow solid, 35 mg, yield: 39.4%. ^{1}H NMR (600 MHz, DMSO-d_6) δ 7.51 (s, 4H), 7.43 (d, *J* = 7.70 Hz, 1H), 7.35 (s, 1H), 7.09 - 7.15 (m, 2H), 6.93 (dt, *J* = 1.10, 7.70 Hz, 1H), 4.26 (s, 2H), 2.23 (s, 3H), 1.33 (s, 9H); ^{13}C NMR (151 MHz, DMSO-d_6) δ 151.6, 143.8, 140.4, 136.8, 134.1, 133.7, 132.7, 131.9, 129.6, 128.2, 125.8, 125.0, 122.4, 118.6, 35.0, 31.5, 20.2, 10.7. HRMS (ESI) calcd for $C_{22}H_{21}N_4$ $[M-H]^-$: 355.1923; found: 355.1924.

5.1.31 (Z)-5-((2-methyl-1-(4-(trifluoromethyl)benzylidene)-1H-inden-3-yl)methyl)-1H-tetrazole (**20f**)

Compound **20f** was synthesized according to the general procedure A. Yellow solid, 35 mg, yield: 38.4%. ^{1}H NMR (600 MHz, DMSO-d_6) δ 7.85 (d, *J* = 7.52 Hz, 2H), 7.76 (d, *J* = 7.89 Hz, 2H), 7.42 (s, 1H), 7.15 (t, *J* = 7.50 Hz, 2H), 7.12 (d, *J* = 6.97 Hz, 1H), 6.92 (dt, *J* = 1.19, 7.38 Hz, 1H), 4.27 (s, 2H), 2.24 (s, 3H); ^{13}C NMR (151 MHz, DMSO-d_6) δ 144.0, 142.2, 141.2, 136.6, 134.0, 133.8, 130.4, 129.9, 129.0, 128.7, 125.9, 125.9, 125.3, 122.5, 118.9, 20.2, 10.6. HRMS (ESI) calcd for $C_{20}H_{14}F_3N_4$ [M-H]$^-$: 367.1171; found: 367.1170.

5.1.32 (Z)-5-((2-methyl-1-(3-(trifluoromethyl)benzylidene)-1H-inden-3-yl)methyl)-1H-tetrazole (**20g**)

Compound **20g** was synthesized according to the general procedure A. Yellow solid, 35 mg, yield: 38.4%. ^{1}H NMR (600 MHz, DMSO-d_6) δ 7.87 (d, *J* = 6.24 Hz, 2H), 7.80 (d, *J* = 7.70 Hz, 1H), 7.74 (t, *J* = 7.98 Hz, 1H), 7.45 (s, 1H), 7.13 - 7.17 (m, 2H), 7.12 (d, *J* = 7.70 Hz, 1H), 6.90 (dt, *J* = 1.00, 7.20 Hz, 1H), 4.27 (s, 2H), 2.24 (s, 3H); ^{13}C NMR (151 MHz, DMSO-d_6) δ 144.1, 142.1, 137.9, 136.6, 133.8, 133.8, 133.6, 130.2, 129.9, 129.8, 128.7, 126.2, 125.3, 125.1, 124.6, 122.2, 118.9, 20.1, 10.6. HRMS (ESI) calcd for $C_{20}H_{14}F_3N_4$ [M-H]$^-$: 367.1171; found: 367.1171.

5.1.33 (Z)-5-((2-methyl-1-(2-(trifluoromethyl)benzylidene)-1H-inden-3-yl)methyl)-1H-tetrazole (**20h**)

Compound **20h** was synthesized according to the general procedure A. Yellow solid, 43 mg, yield: 46.4%. ^{1}H NMR (600 MHz, DMSO-d_6) δ 7.91 (d, *J* = 7.70 Hz, 1H), 7.76 (t, *J* = 7.43 Hz, 1H), 7.68 (t, *J* = 7.70 Hz, 1H), 7.61 (d, *J* = 7.52 Hz, 1H), 7.42 (d, *J* = 1.00 Hz, 1H), 7.12 (d, *J* = 4.22 Hz, 2H), 6.80 - 6.84 (m, 1H), 6.50 (d, *J* = 7.52 Hz, 1H), 4.27 (s, 2H), 2.23 (s, 3H); ^{13}C NMR (151 MHz,

DMSO-d_6) δ 143.9, 142.7, 135.8, 135.7, 134.0, 133.1, 131.7, 129.3, 128.6, 127.3, 127.0, 126.7, 126.6, 125.5, 125.1, 122.6, 118.9, 20.2, 10.5. HRMS (ESI) calcd for $C_{20}H_{14}F_3N_4$ [M-H]$^-$: 367.1171; found: 367.1171.

5.1.34 (Z)-5-((2-methyl-1-(thiophen-2-ylmethylene)-1H-inden-3-yl)methyl)-1H-tetrazole (**20i**)

Compound **20i** was synthesized according to the general procedure A. Yellow solid, 22 mg, yield: 29.4%. ^{1}H NMR (600 MHz, DMSO-d_6) δ 7.94 (d, *J* = 7.70 Hz, 1H), 7.80 (dd, *J* = 1.01, 5.04 Hz, 1H), 7.51 (d, *J* = 3.48 Hz, 1H), 7.38 (s, 1H), 7.23 (dd, *J* = 3.58, 5.04 Hz, 1H), 7.17 (t, *J* = 7.34 Hz, 1H), 7.13 (d, *J* = 7.15 Hz, 1H), 7.04 (dt, *J* = 1.00, 7.20 Hz, 1H), 4.24 (s, 2H), 2.21 (s, 3H); ^{13}C NMR (151 MHz, DMSO-d_6) δ 155.0, 143.8, 140.1, 138.6, 137.0, 133.6, 132.8, 131.7, 129.7, 128.5, 128.4, 125.2, 123.6, 122.7, 118.8, 20.2, 10.8. HRMS (ESI) calcd for $C_{17}H_{13}N_4S$ [M-H]$^-$: 305.0861; found: 305.0862.

5.1.35 (E)-5-((1-(4-isopropylbenzylidene)-1H-inden-3-yl)methyl)-1H-tetrazole (**21a**)

Compound **21a** was synthesized according to the general procedure A. Yellow solid, 47 mg, yield: 57.8%. ^{1}H NMR (600 MHz, DMSO-d_6) δ 7.84 (d, *J* = 7.15 Hz, 1H), 7.37 (s, 1H), 7.33 (d, *J* = 6.97 Hz, 1H), 7.30 (dt, *J* = 1.00, 7.30 Hz, 1H), 7.27 (d, *J* = 7.89 Hz, 2H), 7.22 - 7.26 (m, 2H), 7.19 (d, *J* = 8.07 Hz, 2H), 3.96 (s, 2H), 2.85 (spt, *J* = 6.82 Hz, 1H), 1.18 (d, *J* = 6.97 Hz, 6H); ^{13}C NMR (151 MHz, DMSO-d_6) δ 151.2, 146.8, 145.3, 142.9, 137.4, 136.1, 129.4, 129.3, 126.9, 126.7, 123.9, 120.8, 120.4, 106.9, 33.9, 33.5, 24.4. HRMS (ESI) calcd for $C_{21}H_{19}N_4$ [M-H]$^-$: 327.1610; found: 327.1611.

5.1.36 (E)-5-((1-(4-methoxybenzylidene)-1H-inden-3-yl)methyl)-1H-tetrazole (**21b**)

Compound **21b** was synthesized according to the general procedure A. Yellow solid, 23 mg, yield: 29.3%. ^{1}H NMR (600 MHz, DMSO-d_6) δ 7.83 (dd, *J* = 2.75, 5.69 Hz, 1H), 7.66 (d, *J* = 8.62 Hz, 2H), 7.63 (s, 1H), 7.27 - 7.30 (m, 1H), 7.23 - 7.27 (m, 2H), 7.06 (d, *J* = 8.80 Hz, 2H), 6.99 (s,

1H), 4.38 (s, 2H), 3.82 (s, 3H); ^{13}C NMR (151 MHz, DMSO-d_6) δ 160.4, 141.4, 140.6, 138.6, 136.1, 132.3, 129.4, 129.3, 127.4, 125.9, 124.0, 119.7, 119.4, 115.0, 55.8, 22.7. HRMS (ESI) calcd for $C_{19}H_{15}N_4O$ $[M-H]^-$: 315.1246; found: 315.1246.

5.2 Cell Culture and Transfection

Human breast cancer cell lines MDA-MB-231, were maintained in DMEM containing 10% fetal bovine serum. Human breast cancer cell line MCF-7, and human cervical cancer cell line HeLa were cultured in MEM supplemented 10% fetal bovine serum. These cells were maintained at 5% CO_2 at 37 ℃. Subconfluent cells with exponential growth were used throughout the experiments. Cell transfections were carried out by using Lipofectamine 2000 (Invitrogen) according to the instructions of the manufacturer.

5.3 MTT Assay

Confluent cells cultured in 96-well dishes were treated with various concentrations of compounds for 48 hr. The cells were then incubated with 2 mg/mL 3-(4,5-dimethylthiazol-2-yl)-2,5-diphenyltetrazolium bromide (MTT) for 4 hr at 37 ℃. MTT solution was then aspirated, and formazan in cells was instantly dissolved by addition of 100 μL of DMSO each well. Absorbance was measured at 490 nm.

5.4 Dual-Luciferase Reporter Assay

Cells were transfected with the corresponding plasmids for 24 hours and then treated with compounds for 18 hours. Cells were lysed and Luciferase relative activity was tested by the Dual-Luciferase Reporter Assay System according to the manufacturer's instructions. Transfection effciency was normalized to Renilla luciferase activity.

5.5 Western Blotting

Cell lysates were boiled in sodium dodecyl sulfate (SDS) sample loading buffer, resolved by 10% SDS–polyacrylamide gel electrophoresis (SDS–PAGE) and transferred to nitrocellulose. The membranes were blocked in 5% milk in Tris-buffered saline and Tween 20 (TBST; 10 mM Tris–HCl [pH 8.0], 150 mM NaCl, 0.05% Tween 20) for 1 h at room temperature. After washing twice with TBST, the membranes were incubated with appropriate primary antibodies in TBST for 1 h and then washed thrice at room temperature, probed with horseradish peroxide-linked anti-immunoglobulin. After three washes with TBST, immunoreactive products were visualized using enhanced chemiluminescence reagents and autoradiography.

5.6 Fluorescence quenching

Fluorescence quenching assay was performed using 1 μM of RXRα-PBS solution. Following this, increasing concentrations (0.5 – 35 μM) of the pre-selected 2 compounds were titrated in protein-PBS solution. The fluorescence excitation wavelength set at 280 nm and emission wavelength range of 290–450 nm, at 25°C. Fluorescence emission at the wavelength of maximum intensity (300 nm) was monitored for each concentration of compounds. Fluorescence data were fitted to binding curves using the methods reported [24] for dissociation constant (K_d) calculation. All experiments were performed in triplicates and data were processed using the software Origin 2016.

5.7 Antibody and reagents

Anti-β-actin (Cat. 4970S), and PARP (Cat. 9542) were purchased from Cell Signal Technology (Beverly, MA, USA). RXRα(D-20) (Cat. sc- 553), and GAPDH (Cat. 47724) was purchased from Santa Cruz Biotechnology (Santa Cruz, CA, USA). α- Tubulin (66031-1-lg) was purchased from proteintech. Si-RNA control and Si-RXR from Sigma.

5.8 Molecular docking method

The compounds were prepared by LigPrep module in Maestro 10.5 [25] and was then converted from 2D to 3D with conformation energy minimized using the OPLS3 force field. The crystal structure of RXRα-LBD tetramer retrieved from the Protein Data Bank (www.rcsb.org) (PDB code: 5TBP or 4N8R) was used for the docking study. The protein structure was prepared using Protein Preparation Wizard module in Maestro 10.5, during which hydrogen atoms were added and crystallographic water molecules were removed. Missing side chains and loops were built using Prime in Maestro 10.5 [26]. The binding site was defined based on the positions of crystallized molecules around which the 3D grid box was generated in a size of 15 Å per dimension for docking. Glide in Maestro 10.5 [27] was used for generating the grids and carrying out the docking studies. compounds were docked using the extra precision (XP) mode.

Acknowledgments

This work was supported by the grants from the National Nature Science Fund of China (NSFC-31271453, NSFC-31471318, NSFC-91129302 and NSFC-81301888), the Fundamental Research Funds for the Central Universities (2013121038, 20720180052), the Natural Science Foundation of Fujian Province of China (2018J01133), the National Institutes of Health (CA198982).

References

[1] A. Szanto, V. Narkar, Q. Shen, I.P. Uray, P.J.A. Davies, L. Nagy, Retinoid X receptors: X-ploring their (patho)physiological functions, Cell Death Differ. 11 (2004) S126-S143.

[2] L. Altucci, H. Gronemeyer, The promise of retinoids to fight against cancer, Nat. Rev. Cancer. 1 (2001) 181-193.

[3] J.P. Huang, W.C. Powell, A.C. Khodavirdi, J. Wu, T. Makita, R.D. Cardiff, M.B. Cohen, H.M. Sucov, P. Roy-Burman, Prostatic intraepithelial neoplasia in mice with conditional disruption of the retinoid X receptor alpha allele in the prostate epithelium, Cancer res. 62 (2002) 4812-4819.

[4] M. Li, A.K. Indra, X. Warot, J. Brocard, N. Messaddeq, S. Kato, D. Metzger, P. Chambon, Skin abnormalities generated by temporally controlled RXR alpha mutations in mouse epidermis, Nature. 407 (2000) 633-636.

[5] P. Germain, P. Chambon, G. Eichele, R.M. Evans, M.A. Lazar, M. Leid, A.R. De Lera, R. Lotan, D.J. Mangelsdorf, H. Gronemeyer, International Union of Pharmacology. LXIII. Retinoid

X receptors, Pharmacol Rev. 58 (2006) 760-772.
[6] A. Szanto, V. Narkar, Q. Shen, I.P. Uray, P.J.A. Davies, L. Nagy, Retinoid X receptors: X-ploring their (patho)physiological functions, Cell Death Differ. 11 Suppl 2 (2004) S126.
[7] L. Altucci, M.D. Leibowitz, K.M. Ogilvie, A.R. de Lera, H. Gronemeyer, RAR and RXR modulation in cancer and metabolic disease, Nat. Rev. Drug Discov. 6 (2007) 793-810.
[8] Y. Su, Z. Zeng, Z. Chen, D. Xu, W. Zhang, X.K. Zhang, Recent Progress in the Design and Discovery of RXR Modulators Targeting Alternate Binding Sites of the Receptor, Curr. Top. Med. Chem. 17 (2017) 663-675.
[9] M. Duvic, K. Hymes, P. Heald, D. Breneman, A.G. Martin, P. Myskowski, C. Crowley, R.C. Yocum, G. Bexarotene Worldwide Study, Bexarotene is effective and safe for treatment of refractory advanced-stage cutaneous T-cell lymphoma: Multinational phase II-III trial results, J. Clin. Oncol., 19 (2001) 2456-2471.
[10] M.M. Gottardis, E.D. Bischoff, M.A. Shirley, M.A. Wagoner, W.W. Lamph, R.A. Heyman, Chemoprevention of mammary carcinoma by LGD1069 (Targretin): An RXR-selective ligand, Cancer res. 56 (1996) 5566-5570.
[11] X.K. Zhang, Y. Su, L.Q. Chen, F. Chen, J. Liu, H. Zhou, Regulation of the nongenomic actions of retinoid X receptor-alpha by targeting the coregulator-binding sites, Acta Pharmacol. Sin. 36 (2015) 102-112.
[12] X.K. Zhang, H. Zhou, Y. Su, Targeting truncated RXR alpha for cancer therapy, Acta Biochim. Biophys. Sin. 48 (2016) 49-59.
[13] Z. Zeng, Z. Sun, M. Huang, W. Zhang, J. Liu, L. Chen, F. Chen, Y. Zhou, J. Lin, F. Huang, L. Xu, Z. Zhuang, S. Guo, G. Alitongbieke, G. Xie, Y. Xu, B. Lin, X. Cao, Y. Su, X.-k. Zhang, H. Zhou, Nitrostyrene Derivatives Act as RXR alpha Ligands to Inhibit TNF alpha Activation of NF-kappa B, Cancer res. 75 (2015) 2049-2060.
[14] Y. Katagiri, K. Takeda, Z.X. Yu, V.J. Ferrans, K. Ozato, G. Guroff, Modulation of retinoid signalling through NGF-induced nuclear export of NGFI-B, Nat. Cell Biol. 2 (2000) 435-440.
[15] X.H. Cao, W. Liu, F. Lin, H. Li, S.K. Kolluri, B.Z. Lin, Y.H. Han, M.I. Dawson, X.K. Zhang, Retinoid X receptor regulates Nur77/TR3-dependent apoptosis by modulating its nuclear export and mitochondrial targeting, Mol. Cell. Biol. 25 (2005) 524-524.
[16] F. Balkwill, Tumour necrosis factor and cancer, Nat. Rev. Cancer, 9 (2009) 361-371.
[17] R. Marone, V. Cmiljanovic, B. Giese, M.P. Wymann, Targeting phosphoinositide 3-kinase: moving towards therapy, Biochim. Biophys. Acta, 1784 (2008) 159-185.
[18] E. Pons-Tostivint, B. Thibault, J. Guillermet-Guibert, Targeting PI3K Signaling in Combination Cancer Therapy, Trends in cancer, 3 (2017) 454-469.
[19] H. Zhou, W. Liu, Y. Su, Z. Wei, J. Liu, S.K. Kolluri, H. Wu, Y. Cao, J. Chen, Y. Wu, T. Yan, X. Cao, W. Gao, A. Molotkov, F. Jiang, W.G. Li, B. Lin, H.P. Zhang, J. Yu, S.P. Luo, J.Z. Zeng, G. Duester, P.Q. Huang, X.K. Zhang, NSAID sulindac and its analog bind RXRalpha and inhibit RXRalpha-dependent AKT signaling, Cancer cell, 17 (2010) 560-573.
[20] L. Chen, Z.-G. Wang, A.E. Aleshin, F. Chen, J. Chen, F. Jiang, G. Alitongbieke, Z. Zeng, Y.

Ma, M. Huang, H. Zhou, G. Cadwell, J.-F. Zheng, P.-Q. Huang, R.C. Liddington, X.-k. Zhang, Y. Su, Sulindac-Derived RXR alpha Modulators Inhibit Cancer Cell Growth by Binding to a Novel Site, Chem. Biol. 21 (2014) 596-607.
[21] Z.G. Wang, L. Chen, J. Chen, J.F. Zheng, W. Gao, Z. Zeng, H. Zhou, X.K. Zhang, P.Q. Huang, Y. Su, Synthesis and SAR study of modulators inhibiting tRXRalpha-dependent AKT activation, Eur. J. Med. Chem. 62 (2013) 632-648.
[22] M.J. Walters, A.L. Blobaum, P.J. Kingsley, A.S. Felts, G.A. Sulikowski, L.J. Marnett, The influence of double bond geometry in the inhibition of cyclooxygenases by sulindac derivatives, Bioorg. Med. Chem. Lett., 19 (2009) 3271-3274.
[23] L. Chen, A.E. Aleshin, G. Alitongbieke, Y. Zhou, X. Zhang, X. Ye, M. Hu, G. Ren, Z. Chen, Y. Ma, D. Zhang, S. Liu, W. Gao, L. Cai, L. Wu, Z. Zeng, F. Jiang, J. Liu, H. Zhou, G. Cadwell, R.C. Liddington, Y. Su, X.K. Zhang, Modulation of nongenomic activation of PI3K signalling by tetramerization of N-terminally-cleaved RXRalpha, Nat. Commun. 8 (2017) 16066.
[24] Z.X. Wang, N.R. Kumar, D.K. Srivastava, A novel spectroscopic titration method for determining the dissociation constant and stoichiometry of protein-ligand complex, Anal. Biochem. 206 (1992) 376-381.
[25] Schrödinger Release 2017-1: LigPrep, Schrödinger, LLC, New York, NY, 2017.
[26] Schrödinger Release 2017-1: Prime, Schrödinger, LLC, New York, NY, 2017.
[27] Schrödinger Release 2017-1: Glide, Schrödinger, LLC, New York, NY, 2017.

Highlights:

· Four series of sulindac analogs (a total of 26 compounds) were designed and synthesized.
· Two compounds **8b** and **18a** were identified to have improved binding affinity and apoptotic activity against breast cancer cells.
· **8b** and **18a** can induce the PARP cleavage more potently than K-8008 in a RXRα-dependent manner.